ÖAW AUSTRIAN ACADEMY OF SCIENCES

RICAM – JOHANN RADON INSTITUTE FOR COMPUTATIONAL AND APPLIED MATHEMATICS

Isogeometric analysis with C^1-smooth functions over multi-patch surfaces

A. Farahat, B. Jüttler, M. Kapl, T. Takacs

RICAM-Report 2022-04

Isogeometric analysis with C^1-smooth functions over multi-patch surfaces

Andrea Farahat[a,*], Bert Jüttler[a,b], Mario Kapl[c], Thomas Takacs[a,b]

[a] *Johann Radon Institute for Computational and Applied Mathematics, Austrian Academy of Sciences, Linz, Austria*
[b] *Institute of Applied Geometry, Johannes Kepler University Linz, Linz, Austria*
[c] *Department of Engineering & IT, Carinthia University of Applied Sciences, Villach, Austria*

Abstract

We present a framework for the construction of a globally C^1-smooth isogeometric spline space over a particular class of G^1-smooth multi-patch surfaces called analysis-suitable G^1 (in short AS-G^1) multi-patch surfaces. The class of AS-G^1 multi-patch surfaces consists of those G^1-smooth multi-patch surfaces which allow the construction of C^1-smooth isogeometric spline spaces with optimal polynomial reproduction properties [6]. Our method extends the work [20, 21], which is limited to the case of planar AS-G^1 multi-patch parameterizations, to the case of AS-G^1 multi-patch surfaces. The C^1-smooth isogeometric spline space is generated as the span of locally supported and explicitly given basis functions of three different types that correspond to the patches, interfaces and vertices of the considered AS-G^1 multi-patch surface. We further present simple and practical methods for the design of AS-G^1 multi-patch surfaces and demonstrate the potential of the C^1-smooth spline space for solving fourth order partial differential equations over AS-G^1 multi-patch surfaces on the basis of the biharmonic equation. The obtained numerical results indicate convergence rates of optimal order in the L^2-norm and in the H^1- and H^2-seminorms.

Keywords: Isogeometric analysis, C^1-smooth isogeometric spline space, analysis-suitable G^1 parameterization, multi-patch surface
2010 MSC: 65D07, 65D17, 65N30

1. Introduction

Multi-patch spline surfaces [36] are a powerful tool in computer-aided geometric design [9, 15] to construct complex geometries and can be used in the framework of isogeometric analysis [3, 7, 16] to represent the computational domain of the considered partial differential equation. For solving a fourth order partial differential equation, such as the

*Corresponding author
Email addresses: andrea.farahat@ricam.oeaw.ac.at (Andrea Farahat), bert.juettler@jku.at (Bert Jüttler), m.kapl@fh-kaernten.at (Mario Kapl), thomas.takacs@ricam.oeaw.ac.at (Thomas Takacs)

biharmonic equation, e.g. [2, 6, 18, 22, 33], the Kirchhoff-Love shell problem, e.g. [1, 4, 26–28], the Cahn-Hilliard equation, e.g. [12, 13, 29], or problems of strain gradient elasticity, e.g. [11, 31, 35], over a multi-patch surface directly via its weak form and a standard Galerkin discretization, the multi-patch spline surface has to be G^1-smooth (i.e. geometrically C^1-smooth) and the isogeometric discretization space of the considered problem has to be globally C^1-smooth.

An isogeometric spline function is C^1-smooth over a G^1-smooth multi-patch surface if and only if the associated graph surface is also G^1-smooth [14]. Recall that the graph surface is a two-parametric surface in $\mathbb{R}^4$, whose first three coordinates are the G^1-smooth multi-patch surface and the fourth coordinate is the isogeometric spline function. The equivalence of the C^1-smoothness of the isogeometric function and the G^1-smoothness of the graph of the isogeometric function provides the possibility to construct globally C^1-smooth isogeometric spline spaces over multi-patch surfaces.

The construction of C^1-smooth isogeometric spline spaces for planar multi-patch geometries has been intensively studied in the last years, see e.g., the two recent survey articles [17, 20] for details. For the case of multi-patch surfaces, the existing methods can be roughly classified, similar to the planar case, into three approaches depending on the employed parameterization of the multi-patch surface. The first approach uses a multi-patch parameterization which is C^1-smooth everywhere and which possesses therefore a singularity at extraordinary vertices, see e.g. [34]. In the second technique, the multi-patch parameterization is C^1-smooth everywhere except in the vicinity of an extraordinary vertex where a particular G^1-smooth cap is needed, see e.g. [23–25, 33]. The third approach is based on a multi-patch parameterization which is in general just G^1-smooth across all interfaces, see e.g. [5].

In this work, we follow the third approach to develop a method for the construction of a C^1-smooth isogeometric spline space over a particular class of G^1-smooth multi-patch surfaces, which are called analysis-suitable G^1 (in short, AS-G^1) multi-patch surfaces [6]. The AS-G^1 assumption for a multi-patch surface is required to obtain spaces possessing optimal approximation properties [6, 19]. The constructed C^1-smooth spline space, which is a specific subspace of the full C^1-smooth isogeometric spline space, is easy to generate and possesses the same numerical approximation properties as the full space. We present for the specific C^1-smooth subspace a simple, explicitly given and locally supported basis, which is well suited for numerical simulation. The C^1-smooth subspace is constructed in such a way that its dimension is independent of the underlying AS-G^1 parameterization of the multi-patch surface. Thereby, the proposed approach extends and generalizes the method [20, 21], which is limited to the case of planar AS-G^1 multi-patch parameterizations, in two directions. First, our construction works not only for planar domains but also for AS-G^1 multi-patch surfaces. This requires the adaptation as well as the investigation of different tools used in the construction of the C^1-smooth multi-patch spline space. Second, we introduce the novel concept of an AS-G^1 skeleton, which is the object formed by the topological structure, the connectivity information across the patch interfaces and the neighborhood information of the vertices of an AS-G^1 multi-patch surface. The AS-G^1 skeleton can also be defined and generated without an underlying AS-G^1 multi-patch

surface and is sufficient for the construction of the C^1-smooth multi-patch spline space.

Besides, we also present a novel general framework for the construction of AS-G^1 multi-patch surfaces. The proposed framework is based on the use of a C^1-smooth spline space defined for an appropriately selected AS-G^1 skeleton, and is employed to develop two specific simple and practical design methods. These two techniques are then used to generate some examples of AS-G^1 multi-patch surfaces. The design of AS-G^1 multi-patch surfaces is a challenging task since the desired surfaces have to be not only G^1-smooth, they also have to satisfy the more restrictive AS-G^1 continuity condition. If the AS-G^1 condition is not satisfied, the approximation properties of the isogeometric discretization over the multi-patch surface are, in general, reduced [19].

We further numerically study the approximation properties of the introduced C^1-smooth isogeometric spline space by solving the biharmonic equation over the constructed AS-G^1 multi-patch surfaces. For this purpose, we describe an isogeometric discretization of two different model problems of the biharmonic equation based on the one in [2] for single patch surfaces and homogeneous boundary conditions, and extend it to case of multi-patch surfaces as well as to the case of non-homogeneous boundary conditions. The numerical results indicate optimal approximation properties of the constructed C^1-smooth isogeometric spline space, and show therefore also the great potential of these C^1-smooth functions to solve fourth order partial differential equations over multi-patch surfaces.

The remainder of the paper is organized as follows. In Section 2, we recall some preliminaries, which include the introduction of the used class of multi-patch surfaces, called AS-G^1 multi-patch surfaces (cf. [6]), as well as of the concept of C^1-smooth isogeometric spline spaces over AS-G^1 multi-patch surfaces. In addition, we introduce the concept of the AS-G^1 skeleton of an AS-G^1 multi-patch surface, which is used to generate the specific C^1-smooth isogeometric spline space. Section 3 presents then the construction of this C^1-smooth isogeometric spline space including the construction of a simple, explicitly given and locally supported basis as well as the investigation of the dimension of the C^1-smooth spline space. In Section 4, we describe a novel methodology for the design of AS-G^1 multi-patch surfaces and use it to generate instances of AS-G^1 multi-patch surfaces. Section 5 numerically explores the approximation properties of the introduced C^1-smooth isogeometric spline space by solving the biharmonic equation over the constructed surfaces. For this, we study two different model problems of the biharmonic equation, and establish for both cases an isogeometric Galerkin discretization based on the specific C^1-smooth isogeometric spline space. Finally, we conclude the paper in Section 6.

2. Preliminaries

We first introduce the multi-patch setting which will be used throughout the paper. For this purpose, we consider a particular class of G^1-smooth multi-patch surfaces, called AS-G^1 multi-patch surfaces, which allows the construction of C^1-smooth isogeometric spline spaces with optimal polynomial reproduction properties [6]. In doing so, we follow a similar notation as in [20, 21] for the case of planar multi-patch domains. We also recall the concept of C^1-smooth isogeometric spline spaces over AS-G^1 multi-patch surfaces. Besides this, we

describe further tools, such as the AS-G^1 skeleton, which will be needed among others to construct the C^1-smooth multi-patch spline space in Section 3.

2.1. The multi-patch setting

Let $p \geq 3$, $1 \leq r \leq p-2$ and $k \geq 1$. We denote by $\mathcal{S}_h^{p,r}$ the univariate spline space of degree p, continuity C^r and mesh size $h = \frac{1}{k}$ defined on the parameter domain $[0,1]$, and denote by $\mathcal{S}_h^{\mathbf{p},\mathbf{r}}$, with $\mathbf{p} = (p,p)$ and $\mathbf{r} = (r,r)$, the corresponding bivariate tensor-product spline space $\mathcal{S}_h^{p,r} \otimes \mathcal{S}_h^{p,r}$ defined on the parameter domain $[0,1]^2$. In addition, let $N_j^{p,r}$, $j = 0,\dots,n-1$ with $n = p + (k-1)(p-r) + 1$ the B-splines of the spline space $\mathcal{S}_h^{p,r}$, and let $N_{\mathbf{j}}^{\mathbf{p},\mathbf{r}} = N_{j_1}^{p,r} N_{j_2}^{p,r}$, $\mathbf{j} = (j_1, j_2) \in \{0,\dots,n-1\}^2$, the tensor-product B-splines of the tensor-product spline space $\mathcal{S}_h^{\mathbf{p},\mathbf{r}}$. We also need the univariate spline spaces $\mathcal{S}_h^{p,r+1}$ and $\mathcal{S}_h^{p-1,r}$, where we denote the corresponding B-splines by $N_j^{p,r+1}$, $j = 0,\dots n_0$ with $n_0 = p+(k-1)(p-r-1)+1$, and by $N_j^{p-1,r}$, $j = 0,\dots n_1$ with $n_1 = p+(k-1)(p-r-1)$, respectively. We further introduce basis transformations from $\{N_0^{p,r}, N_1^{p,r}\}$ to $\{M_0^{p,r}, M_1^{p,r}\}$, from $\{N_0^{p,r+1}, N_1^{p,r+1}, N_2^{p,r+1}\}$ to $\{M_0^{p,r+1}, M_1^{p,r+1}, M_2^{p,r+1}\}$ and from $\{N_0^{p-1,r}, N_1^{p-1,r}\}$ to $\{M_0^{p-1,r}, M_1^{p-1,r}\}$, where $M_i^{p,r}$, $i = 0,1$, $M_i^{p,r+1}$, $i = 0,1,2$, and $M_i^{p-1,r}$, $i = 0,1$, are functions with the property that

$$\partial_\xi^j M_i^{p,r}(0) = \delta_i^j \ j = 0,1, \ \partial_\xi^j M_i^{p,r+1}(0) = \delta_i^j \ j = 0,\dots,2, \text{ and } \partial_\xi^j M_i^{p-1,r}(0) = \delta_i^j \ j = 0,1,$$

respectively, and where δ_i^j is the Kronecker delta. The explicit representations of the functions $M_i^{p,r}$, $M_i^{p,r+1}$ and $M_i^{p-1,r}$ are given by

$$M_0^{p,r}(\xi) = \sum_{j=0}^{1} N_j^{p,r}(\xi), \ M_1^{p,r}(\xi) = \frac{h}{p} N_1^{p,r}(\xi),$$

$$M_0^{p,r+1}(\xi) = \sum_{j=0}^{2} N_j^{p,r+1}(\xi), \ M_1^{p,r+1}(\xi) = \frac{h}{p} \sum_{j=1}^{2} \vartheta(j) N_j^{p,r+1}(\xi), \ M_2^{p,r+1}(\xi) = \frac{h^2\mu}{p(p-1)} N_2^{p,r+1}(\xi)$$

with $\vartheta(j) = j$ and $\mu = 1$ for $r < p-2$, and $\vartheta(j) = 2j-1$ and $\mu = 2$ for $r = p-2$, and

$$M_0^{p-1,r}(\xi) = \sum_{j=0}^{1} N_j^{p-1,r}(\xi), \ M_1^{p-1,r}(\xi) = \frac{h}{p} N_1^{p-1,r}(\xi),$$

respectively. Moreover, let $q \geq 1$, then we denote by $\mathcal{P}_1^q$ the univariate space of polynomials of degree q on the parameter domain $[0,1]$, and by $\mathcal{P}_2^{\mathbf{q}}$ with $\mathbf{q} = (q,q)$, the corresponding bivariate tensor-product polynomial space $\mathcal{P}_1^q \otimes \mathcal{P}_1^q$ defined on the parameter domain $[0,1]^2$.

We consider a G^1-smooth[1] conforming[2] multi-patch surface $\mathbf{F}$ consisting of regular quadrilateral surface patch parameterizations $\mathbf{F}^{(i)} \in (\mathcal{S}_h^{\mathbf{p},\mathbf{r}})^3$, $i \in \mathcal{I}_\Omega$. Each parameterization $\mathbf{F}^{(i)}$, $i \in \mathcal{I}_\Omega$, describes via

$$\mathbf{F}^{(i)} : [0,1]^2 \to \overline{\Omega^{(i)}},$$

[1] A multi-patch surface $\mathbf{F}$ is called G^1-smooth if it possesses at each point a well-defined tangent plane, cf. [36].

[2] Here, conforming means that no hanging nodes exists.

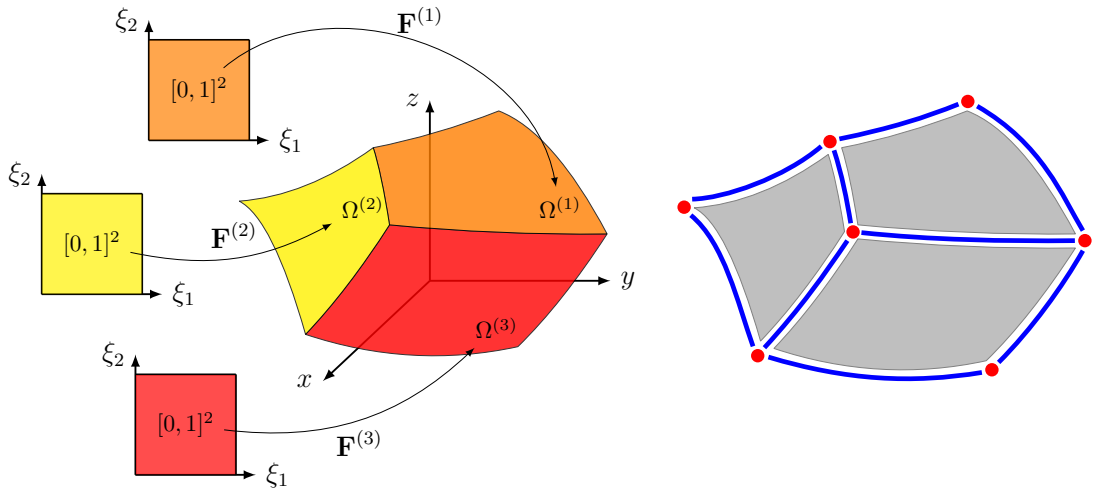

Figure 1: Left: A multi-patch surface domain Ω consisting of three surface patches $\Omega^{(i)}$, $i \in \{1,2,3\}$, with their associated geometry mappings $\mathbf{F}^{(i)}$. Right: The decomposition of the multi-patch surface domain Ω into the individual patches $\Omega^{(i)}$ (gray), curves $\Sigma^{(i)}$ (blue) and vertices $\mathbf{x}^{(i)}$ (red).

a mapping, called the *geometry mapping*. The multi-patch surface $\mathbf{F}$ specifies a surface domain $\Omega \subset \mathbb{R}^3$, which can be represented as the disjoint union of the open quadrilateral surface patches $\Omega^{(i)}$, $i \in \mathcal{I}_\Omega$, of open interface and boundary curves $\Sigma^{(i)}$, $i \in \mathcal{I}_\Sigma$, and of inner and boundary vertices $\mathbf{x}^{(i)}, i \in \mathcal{I}_\chi$, i.e.

$$\Omega = \left(\bigcup_{i \in \mathcal{I}_\Omega} \Omega^{(i)} \right) \cup \left(\bigcup_{i \in \mathcal{I}_\Sigma} \Sigma^{(i)} \right) \cup \left(\bigcup_{i \in \mathcal{I}_\chi} \mathbf{x}^{(i)} \right),$$

where the curves $\Sigma^{(i)}$, $i \in \mathcal{I}_\Sigma$, are in each case the open boundary curve of at least one surface patch parameterization $\mathbf{F}^{(j)}$, $j \in \mathcal{I}_\Omega$, and the vertices $\mathbf{x}^{(i)}, i \in \mathcal{I}_\chi$, are in each case the corner point of at least one surface patch parameterization $\mathbf{F}^{(j)}$, $j \in \mathcal{I}_\Omega$. In addition, we decompose the index sets $\mathcal{I}_\Sigma$ and $\mathcal{I}_\chi$ into $\mathcal{I}_\Sigma = \mathcal{I}_\Sigma^\circ \cup \mathcal{I}_\Sigma^\Gamma$ and $\mathcal{I}_\chi = \mathcal{I}_\chi^\circ \cup \mathcal{I}_\chi^\Gamma$, where $\mathcal{I}_\Sigma^\circ$ and $\mathcal{I}_\Sigma^\Gamma$ are the index sets for all interface and boundary curves $\Sigma^{(i)}$, respectively, and where $\mathcal{I}_\chi^\circ$ and $\mathcal{I}_\chi^\Gamma$ are the index sets for all inner and boundary vertices $\mathbf{x}^{(i)}$, respectively. We further denote by ν_i the patch valence of a vertex $\mathbf{x}^{(i)}$, $i \in \mathcal{I}_\chi$. Note that in case of an inner vertex $\mathbf{x}^{(i)} \in \mathcal{I}_\chi^\circ$ it always holds that $\nu_i \geq 3$.

The patch parameterizations $\mathbf{F}^{(i)}$ induce a connectivity structure on the collection of parameter domains. We denote by $\widehat{\Omega}$ the disjoint union of all parameter domains imbued with the connectivity information, similar to a parameter manifold as in [37], formally we may write

$$\widehat{\Omega} = \{(i, \boldsymbol{\xi}) : i \in \mathcal{I}_\Omega, \boldsymbol{\xi} \in [0,1]^2\} / \sim,$$

where $\sim$ is the equivalence relation, with $(i, \boldsymbol{\xi}) \sim (i', \boldsymbol{\xi}')$, if and only if $\mathbf{F}^{(i)}(\boldsymbol{\xi}) = \mathbf{F}^{(i')}(\boldsymbol{\xi}')$. Note that such an equivalence relation can also be defined without underlying patch parameterizations. In the following we use the same notation for an element $(i, \boldsymbol{\xi})$ and its

equivalence class. We moreover define for each $i \in \mathcal{I}_\Omega$ the subset $\widehat{\Omega}^{(i)} \subset \widehat{\Omega}$ as

$$\widehat{\Omega}^{(i)} = \{(i, \boldsymbol{\xi}) : \boldsymbol{\xi} \in [0,1]^2\}.$$

We also use the simplified notation $\boldsymbol{\xi} \in \widehat{\Omega}^{(i)}$ to signify an element $(i, \boldsymbol{\xi}) \in \widehat{\Omega}^{(i)}$. We can now define a spline space on $\widehat{\Omega}$ as

$$\mathcal{S} = \{f : \widehat{\Omega} \to \mathbb{R} \text{ s.t. } f|_{\widehat{\Omega}^{(i)}} \in \mathcal{S}_h^{\mathbf{p},\mathbf{r}} \text{ for all } i \in \mathcal{I}_\Omega\}.$$

Here $f|_{\widehat{\Omega}^{(i)}}$ is to be interpreted as a function in $\boldsymbol{\xi}$. Thus a C^0-smooth multi-patch surface $\mathbf{F} : \widehat{\Omega} \to \Omega$ is now formally defined as a mapping $\mathbf{F} \in (\mathcal{S})^3$.

An example of a three-patch surface $\mathbf{F}$ consisting of the single surface parameterizations $\mathbf{F}^{(i)}$, $i \in \{1,2,3\}$, as well as the decomposition of the associated three-patch surface domain Ω into the single patches $\Omega^{(i)}$, $i \in \mathcal{I}_\Omega$, curves $\Sigma^{(i)}$, $i \in \mathcal{I}_\Sigma$, and vertices $\mathbf{x}^{(i)}$, $i \in \mathcal{I}_\chi$, is shown in Figure 1.

2.2. Local parameterizations in standard form

To simplify the construction of the C^1-smooth space in Section 3, we locally (re)parameterize in the vicinity of an interface/boundary curve $\Sigma^{(i)}$, $i \in \mathcal{I}_\Sigma$, or in the vicinity of an inner/boundary vertex $\mathbf{x}^{(i)}$, $i \in \mathcal{I}_\chi$, the geometry mappings $\mathbf{F}^{(i_j)}$ of the corresponding surface patches $\Omega^{(i_j)}$ into the so-called *standard form* with respect to the curve $\Sigma^{(i)}$ or vertex $\mathbf{x}^{(i)}$. In the following, let us describe the local parameterizations in standard form for the different possible cases.

In case of an interface curve $\Sigma^{(i)}$, $i \in \mathcal{I}_\Sigma^\circ$, with $\Sigma^{(i)} \subset \overline{\Omega^{(i_1)}} \cap \overline{\Omega^{(i_2)}}$, $i_1, i_2 \in \mathcal{I}_\Omega$, the two associated geometry mappings $\mathbf{F}^{(i_1)}$ and $\mathbf{F}^{(i_2)}$ are (re)parameterized in such a way that the common interface curve $\Sigma^{(i)}$ is given by

$$\mathbf{F}^{(i_1)}(0,\xi) = \mathbf{F}^{(i_2)}(\xi,0), \quad \xi \in (0,1), \tag{1}$$

see Figure 2 (left). Similarly, for a boundary curve $\Sigma^{(i)}$, $i \in \mathcal{I}_\Sigma^\Gamma$, with $\Sigma^{(i)} \subset \overline{\Omega^{(i_1)}}$, $i_1 \in \mathcal{I}_\Omega$, we (re)parameterize the associated geometry mapping $\mathbf{F}^{(i_1)}$ in such a way that the boundary curve $\Sigma^{(i)}$ is given by

$$\Sigma^{(i)} = \{\mathbf{F}^{(i_1)}(0,\xi) \,:\, \xi \in (0,1)\},$$

see Figure 2 (right).

In case of an inner vertex $\mathbf{x}^{(i)}$, $i \in \mathcal{I}_\chi^\circ$, with patch valence ν_i, we label the patches and interface curves around the vertex $\mathbf{x}^{(i)}$ in counterclockwise order as $\Sigma^{(i_1)}$, $\Omega^{(i_2)}$, $\Sigma^{(i_3)}$, ..., $\Sigma^{(i_{2\nu_i-1})}$, $\Omega^{(i_{2\nu_i})}$, cf. Figure 3 (left), and further set $\Sigma^{(i_{2\nu_i+1})} = \Sigma^{(i_1)}$ and $\Omega^{(i_0)} = \Omega^{(i_{2\nu_i})}$. We (re)parameterize the associated geometry mappings $\mathbf{F}^{(i_{2k})}$, $k = 1, \ldots, \nu_i$, in such a way that each interface curve $\Sigma^{(i_{2k+1})}$, $k = 1, \ldots, \nu_i - 1$, is given by

$$\mathbf{F}^{(i_{2k})}(0,\xi) = \mathbf{F}^{(i_{2k+2})}(\xi,0), \ \xi \in (0,1),$$

and that the remaining interface curve $\Sigma^{(i_1)}$ is given by

$$\mathbf{F}^{(i_{2\nu_i})}(0,\xi) = \mathbf{F}^{(i_2)}(\xi,0), \ \xi \in (0,1),$$

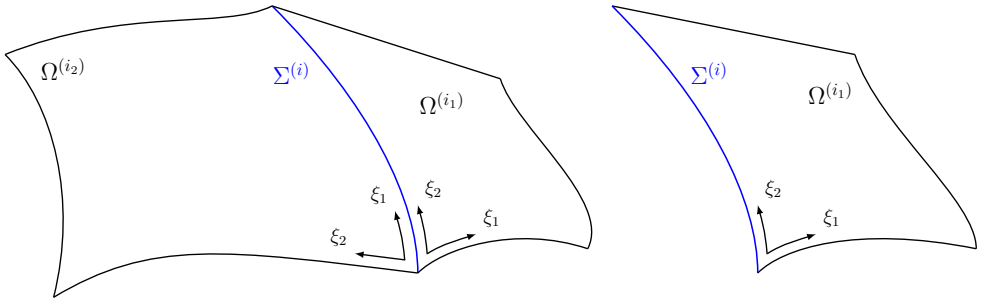

Figure 2: Left: Parameterization of the two neighboring surface patches $\Omega^{(i_1)}$ and $\Omega^{(i_2)}$ in standard form with respect to their common interface curve $\Sigma^{(i)}$. Right: Parameterization of the surface patch $\Omega^{(i_1)}$ in standard form with respect to the boundary curve $\Sigma^{(i)}$.

which implies that

$$\mathbf{x}^{(i)} = \mathbf{F}^{(i_2)}(0,0) = \mathbf{F}^{(i_4)}(0,0) = \ldots = \mathbf{F}^{(i_{2\nu_i})}(0,0),$$

cf. Figure 3 (left).

Similarly, we can perform a local (re)parameterization in standard form with respect to a boundary vertex $\mathbf{x}^{(i)}$, $i \in \mathcal{I}_\chi^\Gamma$, with a patch valence $\nu_i \geq 1$. For this purpose, we label the patches and interface/boundary curves around the vertex $\mathbf{x}^{(i)}$ in counterclockwise order as $\Sigma^{(i_1)}$, $\Omega^{(i_2)}$, $\Sigma^{(i_3)}$, $\ldots$, $\Sigma^{(i_{2\nu_i-1})}$, $\Omega^{(i_{2\nu_i})}$, $\Sigma^{(i_{2\nu_i+1})}$, cf. Figure 3 (right), where $\Sigma^{(i_1)}$ and $\Sigma^{(i_{2\nu_i+1})}$ are boundary curves and $\Sigma^{(i_{2k+1})}$, $k = 1, \ldots, \nu_i - 1$, are interface curves. Then, the associated geometry mappings $\mathbf{F}^{(i_{2k})}$, $k = 1, \ldots, \nu_i$, are (re)parameterized in such a way that each interface curve $\Sigma^{(i_{2k+1})}$, $k = 1, \ldots, \nu_i - 1$, is given by

$$\mathbf{F}^{(i_{2k})}(0,\xi) = \mathbf{F}^{(i_{2k+2})}(\xi,0), \ \xi \in (0,1),$$

which leads again to

$$\mathbf{x}^{(i)} = \mathbf{F}^{(i_2)}(0,0) = \mathbf{F}^{(i_4)}(0,0) = \ldots = \mathbf{F}^{(i_{2\nu_i})}(0,0),$$

cf. Figure 3 (right).

2.3. Tools & operators for G^1-smooth multi-patch surfaces

We need for the G^1-smooth multi-patch surface $\mathbf{F}$ (and hence for its surface domain Ω) specific tools and (differential) operators, which have been already studied for the single-patch case in [2]. Let us consider first an arbitrary surface patch $\Omega^{(i)}$, $i \in \mathcal{I}_\Omega$, with its geometry mapping $\mathbf{F}^{(i)}$, and let us denote by $\boldsymbol{\xi} = (\xi_1, \xi_2)$ the coordinates with respect to the parameter domain $[0,1]^2$. We define for the patch parameterization $\mathbf{F}^{(i)}$ the Jacobian $J^{(i)} : [0,1]^2 \to \mathbb{R}^{3\times 2}$ as

$$J^{(i)}(\xi_1,\xi_2) = \left[\partial_1 \mathbf{F}^{(i)}(\xi_1,\xi_2) \quad \partial_2 \mathbf{F}^{(i)}(\xi_1,\xi_2)\right], \tag{2}$$

the coefficients $G^{(i)} : [0,1]^2 \to \mathbb{R}^{2\times 2}$ of the first fundamental form as

$$G^{(i)}(\boldsymbol{\xi}) = \left(J^{(i)}(\boldsymbol{\xi})\right)^T J^{(i)}(\boldsymbol{\xi}), \tag{3}$$

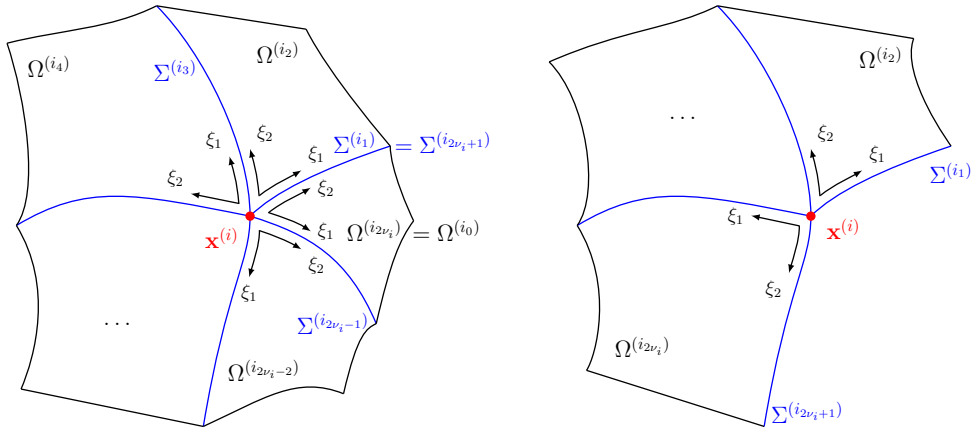

Figure 3: Left: Parameterization of surface patches $\Omega^{(i_2)}$, ..., $\Omega^{(i_{2\nu_i})}$ in standard form with respect to their common inner vertex $\mathbf{x}^{(i)}$. Right: Parameterization of surface patches $\Omega^{(i_2)}$, ..., $\Omega^{(i_{2\nu_i})}$ in standard form with respect to their common boundary vertex $\mathbf{x}^{(i)}$.

and the square root $g^{(i)} : [0,1]^2 \to \mathbb{R}$ of the determinant of $G^{(i)}$ as

$$g^{(i)}(\boldsymbol{\xi}) = \sqrt{\det\left(G^{(i)}(\boldsymbol{\xi})\right)}. \tag{4}$$

Let $\phi^{(i)} \in C^2(\Omega^{(i)})$, and let $\mathbf{v}^{(i)} \in \left[C^1(\Omega^{(i)})\right]^3$ be a vector field. We write

$$\phi^{(i)}(\mathbf{x}) = \left(\psi^{(i)} \circ (\mathbf{F}^{(i)})^{-1}\right)(\mathbf{x}), \quad \mathbf{x} \in \Omega^{(i)},$$

with $\psi^{(i)}(\boldsymbol{\xi}) = \left(\phi^{(i)} \circ \mathbf{F}^{(i)}\right)(\boldsymbol{\xi})$, and

$$\mathbf{v}^{(i)}(\mathbf{x}) = \left(\mathbf{w}^{(i)} \circ (\mathbf{F}^{(i)})^{-1}\right)(\mathbf{x}), \quad \mathbf{x} \in \Omega^{(i)},$$

with $\mathbf{w}^{(i)}(\boldsymbol{\xi}) = \left(\mathbf{v}^{(i)} \circ \mathbf{F}^{(i)}\right)(\boldsymbol{\xi})$. Thanks to the invertibility of the geometry mapping $\mathbf{F}^{(i)}$ and to the equations (2), (3) and (4), the surface gradient $\nabla_{\Omega^{(i)}}\phi^{(i)}$, the surface divergence $\nabla_{\Omega^{(i)}} \cdot \mathbf{v}^{(i)}$ and the Laplace-Beltrami operator $\Delta_{\Omega^{(i)}}\phi^{(i)}$ over the surface patch $\Omega^{(i)}$ can be computed via

$$\nabla_{\Omega^{(i)}}\phi^{(i)}(\mathbf{x}) = \left[J^{(i)}(G^{(i)})^{-1}\nabla_{\boldsymbol{\xi}}\psi^{(i)}\right] \circ (\mathbf{F}^{(i)})^{-1}(\mathbf{x}), \quad \mathbf{x} \in \Omega^{(i)},$$

$$\nabla_{\Omega^{(i)}} \cdot \mathbf{v}^{(i)}(\mathbf{x}) = \left[\frac{1}{g^{(i)}}\nabla_{\boldsymbol{\xi}} \cdot \left((G_0^{(i)})^{-1}(\mathbf{F}^{(i)})^T\mathbf{w}^{(i)}\right)\right] \circ (\mathbf{F}^{(i)})^{-1}(\mathbf{x}), \quad \mathbf{x} \in \Omega^{(i)},$$

and

$$\Delta_{\Omega^{(i)}}\phi^{(i)}(\mathbf{x}) = \nabla_{\Omega^{(i)}} \cdot (\nabla_{\Omega^{(i)}}\phi^{(i)}(\mathbf{x})) = \left[\frac{1}{g^{(i)}}\nabla_{\boldsymbol{\xi}} \cdot \left((G_0^{(i)})^{-1}\nabla_{\boldsymbol{\xi}}\psi^{(i)}\right)\right] \circ (\mathbf{F}^{(i)})^{-1}(\mathbf{x}), \quad \mathbf{x} \in \Omega^{(i)},$$

respectively, where $\nabla_{\boldsymbol{\xi}}$ is the gradient with respect to the coordinates $\boldsymbol{\xi}$ and where

$$G_0^{(i)}(\boldsymbol{\xi}) = \frac{1}{g^{(i)}(\boldsymbol{\xi})}G^{(i)}(\boldsymbol{\xi}).$$

Let us consider now a function ϕ on Ω with $\phi|_{\Omega^{(i)}} \in C^2(\Omega^{(i)})$, $i \in \mathcal{I}_\Omega$, and a vector field $\mathbf{v}$ over Ω with $\mathbf{v}|_{\Omega^{(i)}} \in \left[C^1(\Omega^{(i)})\right]^3$, $i \in \mathcal{I}_\Omega$. Then, the surface gradient $\nabla_\Omega \phi$, the surface divergence $\nabla_\Omega \cdot \mathbf{v}$ and the Laplace-Beltrami operator $\Delta_\Omega \phi$ over the entire multi-patch surface Ω is just the collection of the single surface gradients $\nabla_{\Omega^{(i)}} \phi|_{\Omega^{(i)}}$, $i \in \mathcal{I}_\Omega$, the collection of the single surface divergences $\nabla_{\Omega^{(i)}} \cdot \mathbf{v}|_{\Omega^{(i)}}$, $i \in \mathcal{I}_\Omega$, and the collection of the single Laplace-Beltrami operators $\Delta_{\Omega^{(i)}} \phi|_{\Omega^{(i)}}$, $i \in \mathcal{I}_\Omega$, respectively.

2.4. The class of AS-G^1 multi-patch surfaces and their skeletons

It is well-known that a C^0-smooth multi-patch surface $\mathbf{F}$ is G^1-smooth if and only if for any two neighboring patches $\Omega^{(i_1)}$ and $\Omega^{(i_2)}$, $i_1, i_2 \in \mathcal{I}_\Omega$, parameterized via the geometry mappings $\mathbf{F}^{(i_1)}$ and $\mathbf{F}^{(i_2)}$ in standard form with respect to the common interface curve $\Sigma^{(i)} \subset \overline{\Omega^{(i_1)}} \cap \overline{\Omega^{(i_2)}}$, cf. Figure 2 (left), there exists functions $\alpha^{(i,i_1)} : [0,1] \to \mathbb{R}$, $\alpha^{(i,i_2)} : [0,1] \to \mathbb{R}$ and $\beta^{(i)} : [0,1] \to \mathbb{R}$ satisfying

$$\alpha^{(i,i_1)}(\xi)\, \alpha^{(i,i_2)}(\xi) > 0, \quad \xi \in [0,1],$$

and

$$\alpha^{(i,i_1)}(\xi)\, \partial_2 \mathbf{F}^{(i_2)}(\xi,0) + \alpha^{(i,i_2)}(\xi)\, \partial_1 \mathbf{F}^{(i_1)}(0,\xi) + \beta^{(i)}(\xi)\, \partial_2 \mathbf{F}^{(i_1)}(0,\xi) = \mathbf{0}, \quad \xi \in [0,1], \tag{5}$$

cf. [36]. Note that the functions $\alpha^{(i,i_1)}$, $\alpha^{(i,i_2)}$ and $\beta^{(i)}$ are uniquely determined up to a common function $\gamma^{(i)} : [0,1] \to \mathbb{R}$.

In this work, we are interested in a particular class of G^1-smooth multi-patch surfaces, called AS-G^1 multi-patch surfaces. The definition of the class of AS-G^1 multi-patch surfaces is as follows [6]: A G^1-smooth multi-patch surface $\mathbf{F}$ is analysis-suitable G^1 (in short AS-G^1), if for each interface curve $\Sigma^{(i)}$, $i \in \mathcal{I}_\Sigma^{(i)}$, the functions $\alpha^{(i,i_1)}$ and $\alpha^{(i,i_2)}$ are linear polynomials and if there further exists linear polynomials $\beta^{(i,i_1)} : [0,1] \to \mathbb{R}$ and $\beta^{(i,i_2)} : [0,1] \to \mathbb{R}$ such that

$$\beta^{(i)}(\xi) = \alpha^{(i,i_1)}(\xi)\, \beta^{(i,i_2)}(\xi) + \alpha^{(i,i_2)}(\xi)\, \beta^{(i,i_1)}(\xi) \quad \xi \in [0,1]. \tag{6}$$

Note that the linear polynomials $\beta^{(i,i_1)}$ and $\beta^{(i,i_2)}$ are in general not uniquely determined [6].

To obtain uniquely determined functions $\alpha^{(i,i_1)}$, $\alpha^{(i,i_2)}$, $\beta^{(i,i_1)}$ and $\beta^{(i,i_2)}$ for each interface curve $\Sigma^{(i)}$, $i \in \mathcal{I}_\Sigma^\circ$, we select these functions in such a way that the functions $\alpha^{(i,i_1)}$ and $\alpha^{(i,i_2)}$ are relatively prime and minimize

$$||\alpha^{(i,i_1)} - 1||^2_{L_2([0,1])} + ||\alpha^{(i,i_2)} - 1||^2_{L_2([0,1])},$$

and that the functions $\beta^{(i,i_1)}$ and $\beta^{(i,i_2)}$ minimize

$$||\beta^{(i,i_1)}||^2_{L_2([0,1])} + ||\beta^{(i,i_2)}||^2_{L_2([0,1])},$$

cf. [21]. In case of parametric C^1 continuity across the interface curve $\Sigma^{(i)}$, i.e. $\beta^{(i)} \equiv 0$ and $\alpha^{(i,i_1)} = \alpha^{(i,i_2)}$, this would then lead just to $\beta^{(i,i_1)} = \beta^{(i,i_2)} \equiv 0$ and $\alpha^{(i,i_1)} \equiv \alpha^{(i,i_2)} \equiv 1$. The functions $\alpha^{(i,i_1)}$, $\alpha^{(i,i_2)}$, $\beta^{(i,i_1)}$ and $\beta^{(i,i_2)}$ are also called the *gluing data*.

We collect the gluing data for all interfaces in the set

$$\mathcal{G} = \{((i_1, i_2), \alpha^{(i,i_1)}, \alpha^{(i,i_2)}, \beta^{(i,i_1)}, \beta^{(i,i_2)})_i : i \in \mathcal{I}_\Sigma^\circ\}.$$

Thus, the gluing data $\mathcal{G}$ encodes the entire G^1-smoothness information of the multi-patch surface $\mathbf{F}$, as specified by (5)-(6) for a single interface in standard form.

Moreover, we collect the second order Taylor expansions of all patches around each vertex, that is

$$\mathcal{T} = \left\{ \left((i_2, i_4, \dots, i_{2\nu_i}), \mathbf{F}_T^{(i_2)}, \mathbf{F}_T^{(i_4)}, \dots, \mathbf{F}_T^{(i_{2\nu_i})} \right)_i : i \in \mathcal{I}_\chi \right\},$$

with $\mathbf{F}_T^{(i_{2k})} \in (\mathcal{P}_2^2)^3$ and $k = 1, \dots, \nu_i$. Here we denote by $\mathcal{P}_2^2$ the space of bivariate polynomials of total degree ≤ 2. If the vertex is in standard form, we have

$$\partial_1^{\ell_1} \partial_2^{\ell_2} \mathbf{F}^{(i_{2k})}(0,0) = \partial_1^{\ell_1} \partial_2^{\ell_2} \mathbf{F}_T^{(i_{2k})}(0,0)$$

for all $\ell_1, \ell_2 \in \mathbb{Z}_0^+$ with $\ell_1 + \ell_2 \leq 2$. We define the *AS-G^1 skeleton* of the multi-patch surface $\mathbf{F}$ as

$$\mathcal{M} = (\widehat{\Omega}, \mathcal{G}, \mathcal{T}).$$

Note that a skeleton can be defined without any underlying multi-patch surface. However, it is not clear which collection of local patches, AS-G^1 gluing data and second order vertex data actually allows the definition of a multi-patch surface, such that each patch parameterization is regular. A necessary condition is that the local, second order vertex data must be consistent with the gluing data, i.e., that the pairs of neighboring Taylor expansions satisfy (5). The study of these consistency relations between interface gluing data and second order vertex data will be the topic of future research. We assume from now on that any skeleton is consistent, which is, e.g., the case if it is computed from a given AS-G^1 multi-patch parameterization.

The design of AS-G^1 multi-patch parameterizations has been considered so far mainly for the case of planar domains, see e.g. [6, 18–20]. As an exception, the method [19] has also been used to generate a single example of an AS-G^1 multi-patch surface. In Section 4, we will extend this approach by a novel methodology to construct AS-G^1 multi-patch surfaces.

2.5. The space of C^1-smooth isogeometric spline functions

Considering a multi-patch surface $\mathbf{F} \in (\mathcal{S})^3$, with $\mathbf{F}(\widehat{\Omega}) = \Omega$, the space of isogeometric spline functions over Ω is given as

$$\mathcal{V} = \left\{ \varphi \in C^0(\Omega) \ : \ \varphi \circ \mathbf{F} \in \mathcal{S} \right\}.$$

In the following we consider $\mathbf{F}$ to be an AS-G^1 multi-patch surface. Then the space of C^1-smooth isogeometric spline functions over $\mathbf{F}$ is defined as

$$\mathcal{V}^1 = \mathcal{V} \cap C^1(\Omega).$$

We have by definition

$$\mathcal{V}^1 = \left\{ \varphi \in C^1(\Omega) \ : \ \varphi \circ \mathbf{F}^{(i)} \in \mathcal{S}_h^{\mathbf{p},\mathbf{r}}, \ i \in \mathcal{I}_\Omega \right\}.$$

The space $\mathcal{V}^1$ can be characterized by means of the graph $\mathbf{\Phi} \subset \Omega \times \mathbb{R}$ of an isogeometric function $\varphi \in \mathcal{V}$, which is the collection of the single graph surface patches $\mathbf{\Phi}^{(i)} : [0,1]^2 \to \Omega^{(i)} \times \mathbb{R}$, $i \in \mathcal{I}_\Omega$, given by

$$\mathbf{\Phi}^{(i)}(\xi_1, \xi_2) = \left[\mathbf{F}^{(i)}(\xi_1, \xi_2) \quad f^{(i)}(\xi_1, \xi_2) \right]^T,$$

with $f^{(i)} = \varphi \circ \mathbf{F}^{(i)}$. Then, an isogeometric function $\varphi \in \mathcal{V}$ belongs to the space $\mathcal{V}^1$ if and only if the associated graph $\mathbf{\Phi}$ is G^1-smooth [14]. In our multi-patch setting, the graph $\mathbf{\Phi}$ of an isogeometric function $\varphi \in \mathcal{V}$ is G^1-smooth if and only if for any two neighboring patches $\Omega^{(i_1)}$ and $\Omega^{(i_2)}$, $i_1, i_2 \in \mathcal{I}_\Omega$, assuming that the two geometry mappings $\mathbf{F}^{(i_1)}$ and $\mathbf{F}^{(i_2)}$ are given in standard form with respect to the common interface curve $\Sigma^{(i)} \subset \overline{\Omega^{(i_1)}} \cap \overline{\Omega^{(i_2)}}$, cf. Figure 2 (left) and Section 2.2, the two associated graph surface patches $\mathbf{\Phi}^{(i_1)}$ and $\mathbf{\Phi}^{(i_2)}$ satisfy

$$\mathbf{\Phi}^{(i_1)}(0, \xi) = \mathbf{\Phi}^{(i_2)}(\xi, 0), \quad \xi \in [0,1], \tag{7}$$

and

$$\alpha^{(i,i_1)}(\xi) \, \partial_2 \mathbf{\Phi}^{(i_2)}(\xi, 0) + \alpha^{(i,i_2)}(\xi) \, \partial_1 \mathbf{\Phi}^{(i_1)}(0, \xi) + \beta^{(i)}(\xi) \, \partial_2 \mathbf{\Phi}^{(i_1)}(0, \xi) = \mathbf{0}, \quad \xi \in [0,1]. \tag{8}$$

Since $\mathbf{F}$ is an AS-G^1 multi-patch surface, the equations obtained by considering the first three coordinates in equations (7) and (8) are trivially satisfied by (1) and (5), respectively, and we directly obtain: An isogeometric function $\varphi \in \mathcal{V}$ belongs to the space $\mathcal{V}^1$, that is, the function φ is C^1-smooth on Ω, if and only if for any two neighboring patches $\Omega^{(i_1)}$ and $\Omega^{(i_2)}$, $i_1, i_2 \in \mathcal{I}_\Omega$, assuming that the two geometry mappings $\mathbf{F}^{(i_1)}$ and $\mathbf{F}^{(i_2)}$ are given in standard form with respect to the common interface curve $\Sigma^{(i)} \subset \overline{\Omega^{(i_1)}} \cap \overline{\Omega^{(i_2)}}$, cf. Figure 2 (left) and Section 2.2, the two associated spline functions $f^{(i_1)} = \varphi \circ \mathbf{F}^{(i_1)}$ and $f^{(i_2)} = \varphi \circ \mathbf{F}^{(i_2)}$ fulfill

$$f^{(i_1)}(0, \xi) = f^{(i_2)}(\xi, 0), \quad \xi \in [0,1], \tag{9}$$

and

$$\alpha^{(i,i_1)}(\xi) \, \partial_2 f^{(i_2)}(\xi, 0) + \alpha^{(i,i_2)}(\xi) \, \partial_1 f^{(i_1)}(0, \xi) + \beta^{(i)}(\xi) \, \partial_2 f^{(i_1)}(0, \xi) = 0, \quad \xi \in [0,1]. \tag{10}$$

Using equations (6) and (9), equation (10) is further equivalent to

$$\frac{\partial_1 f^{(i_1)}(0, \xi) + \beta^{(i,i_1)}(\xi) \partial_2 f^{(i_1)}(0, \xi)}{\alpha^{(i,i_1)}(\xi)} = -\frac{\partial_2 f^{(i_2)}(\xi, 0) + \beta^{(i,i_2)}(\xi) \partial_1 f^{(i_2)}(\xi, 0)}{\alpha^{(i,i_2)}(\xi)}, \quad \xi \in [0,1]. \tag{11}$$

3. A C^1-smooth isogeometric spline space defined by a skeleton

We present the design of a particular C^1-smooth isogeometric spline space, which is constructed from an AS-G^1 skeleton $\mathcal{M}$. It extends the construction of the C^1-smooth

multi-patch spline space [20, 21], which is limited to the planar case, to the surface case. The obtained C^1-smooth isogeometric spline space is a subspace of the full C^1-smooth spline space $\mathcal{V}^1$, is simpler to generate, has a dimension which depends only on p, r, h and the multi-patch topology and possesses optimal approximation properties as the numerical results in Section 5.2 indicate.

The idea is to generate a C^1-smooth isogeometric spline space $\mathcal{A} \subset \mathcal{V}^1$, which is given by the direct sum

$$\mathcal{A} = \left(\bigoplus_{i \in \mathcal{I}_\Omega} \mathcal{A}_{\Omega^{(i)}} \right) \oplus \left(\bigoplus_{i \in \mathcal{I}_\Sigma} \mathcal{A}_{\Sigma^{(i)}} \right) \oplus \left(\bigoplus_{i \in \mathcal{I}_\chi} \mathcal{A}_{\mathbf{x}^{(i)}} \right), \tag{12}$$

where the spaces $\mathcal{A}_{\Omega^{(i)}}$, $\mathcal{A}_{\Sigma^{(i)}}$ and $\mathcal{A}_{\mathbf{x}^{(i)}}$ are called patch, edge and vertex function spaces, respectively, and correspond to the single patches $\Omega^{(i)}$, $i \in \mathcal{I}_\Omega$, edges (i.e. interface and boundary curves) $\Sigma^{(i)}$, $i \in \mathcal{I}_\Sigma$, and vertices $\mathbf{x}^{(i)}$, $i \in \mathcal{I}_\chi$, respectively. The construction of the C^1-smooth space $\mathcal{A}$ will need a small enough mesh size h, namely selected as $h \leq \frac{p-r-1}{4-r}$.

Below, we first describe in detail the construction of the different spaces. While the design of the patch function space $\mathcal{A}_{\Omega^{(i)}}$ and of the edge function space $\mathcal{A}_{\Sigma^{(i)}}$ works analogously to the planar case [20, 21], the construction of the vertex function space $\mathcal{A}_{\mathbf{x}^{(i)}}$ requires some adaptations. We define each space via its pullback to the parameter domain $\widehat{\Omega}$, denoted with a $\widehat{\cdot}$, i.e., $\widehat{\mathcal{A}} = \{f : \widehat{\Omega} \to \mathbb{R} \mid f \circ \mathbf{F}^{-1} \in \mathcal{A}\} \subset \mathcal{S}$.

3.1. Patch function space

Let $i \in \mathcal{I}_\Omega$. We define the associated patch function space $\widehat{\mathcal{A}}_{\Omega^{(i)}} : \widehat{\Omega} \to \mathbb{R}$ as

$$\widehat{\mathcal{A}}_{\Omega^{(i)}} = \operatorname{span}\{\widehat{\phi}_{\Omega^{(i)},\mathbf{j}} : \mathbf{j} \in \{2, \dots, n-3\}^2\}$$

with

$$\widehat{\phi}_{\Omega^{(i)},\mathbf{j}}(\boldsymbol{\xi}) = \begin{cases} N_{\mathbf{j}}^{\mathbf{p},\mathbf{r}}(\boldsymbol{\xi}) & \text{if } \boldsymbol{\xi} \in \widehat{\Omega}^{(i)}, \\ 0 & \text{otherwise.} \end{cases}$$

Given a skeleton $\mathcal{M} = (\widehat{\Omega}, \mathcal{G}, \mathcal{T})$, the patch function spaces depend only on $\widehat{\Omega}$ and are independent of the edge gluing data $\mathcal{G}$ and vertex data $\mathcal{T}$.

3.2. Edge function space

We distinguish between the case of an interface, that is, $i \in \mathcal{I}_\Sigma^\circ$, and of a boundary curve, that is, $i \in \mathcal{I}_\Sigma^\Gamma$, of the multi-patch surface domain Ω. Let first $i \in \mathcal{I}_\Gamma^\circ$ correspond to an interface, such that its two neighboring patches have the indices $i_1, i_2 \in \mathcal{I}_\Omega$. We assume that the patches are given in standard form with respect to the interface, cf. Figure 2 (left) and Section 2.2. The corresponding edge function space $\widehat{\mathcal{A}}_{\Sigma^{(i)}}$ is defined as

$$\widehat{\mathcal{A}}_{\Sigma^{(i)}} = \operatorname{span}\{\widehat{\phi}_{\Sigma^{(i)},(j_1,j_2)} :\ j_1 \in \{3 - j_2, \dots, n_{j_2} - 4 + j_2\},\ j_2 \in \{0, 1\}\}$$

with

$$\widehat{\phi}_{\Sigma^{(i)},(j_1,j_2)}(\boldsymbol{\xi}) = \begin{cases} f^{(i_1)}_{\Gamma^{(i)},(j_1,j_2)}(\boldsymbol{\xi}) & \text{if } \boldsymbol{\xi} \in \widehat{\Omega}^{(i_1)}, \\ f^{(i_2)}_{\Gamma^{(i)},(j_1,j_2)}(\boldsymbol{\xi}) & \text{if } \boldsymbol{\xi} \in \widehat{\Omega}^{(i_2)}, \\ 0 & \text{otherwise,} \end{cases}$$

where

$$f^{(i_1)}_{\Sigma^{(i)},(j_1,0)}(\xi_1,\xi_2) = N^{p,r+1}_{j_1}(\xi_2)M^{p,r}_0(\xi_1) - \beta^{(i,i_1)}(\xi_2)\left(N^{p,r+1}_{j_1}\right)'(\xi_2)M^{p,r}_1(\xi_1),$$
$$f^{(i_2)}_{\Sigma^{(i)},(j_1,0)}(\xi_1,\xi_2) = N^{p,r+1}_{j_1}(\xi_1)M^{p,r}_0(\xi_2) - \beta^{(i,i_2)}(\xi_1)\left(N^{p,r+1}_{j_1}\right)'(\xi_1)M^{p,r}_1(\xi_2),$$

and

$$f^{(i_1)}_{\Sigma^{(i)},(j_1,1)}(\xi_1,\xi_2) = \alpha^{(i,i_1)}(\xi_2)N^{p-1,r}_{j_1}(\xi_2)N^{p,r}_1(\xi_1),$$
$$f^{(i_2)}_{\Sigma^{(i)},(j_1,1)}(\xi_1,\xi_2) = -\alpha^{(i,i_2)}(\xi_1)N^{p-1,r}_{j_1}(\xi_1)N^{p,r}_1(\xi_2).$$

Let now $i \in \mathcal{I}^{\Gamma}_{\Sigma}$ correspond to a boundary curve of the patch with index $i_1 \in \mathcal{I}_{\Omega}$. Assume again that the patch is given in standard form with respect to the boundary curve, cf. Figure 2 (right) and Section 2.2. The associated edge function space $\widehat{\mathcal{A}}_{\Sigma^{(i)}}$ is given by

$$\widehat{\mathcal{A}}_{\Sigma^{(i)}} = \operatorname{span}\{\widehat{\phi}_{\Sigma^{(i)},(j_1,j_2)} :\ j_1 \in \{3-j_2,\dots,n_{j_2}-4+j_2\},\ j_2 \in \{0,1\}\}$$

with

$$\widehat{\phi}_{\Sigma^{(i)},(j_1,j_2)}(\boldsymbol{\xi}) = \begin{cases} f^{(i_1)}_{\Gamma^{(i)},(j_1,j_2)}(\boldsymbol{\xi}) & \text{if } \boldsymbol{\xi} \in \widehat{\Omega}^{(i_1)}, \\ 0 & \text{otherwise,} \end{cases}$$

where again

$$f^{(i_1)}_{\Sigma^{(i)},(j_1,0)}(\xi_1,\xi_2) = N^{p,r+1}_{j_1}(\xi_2)M^{p,r}_0(\xi_1) - \beta^{(i,i_1)}(\xi_2)\left(N^{p,r+1}_{j_1}\right)'(\xi_2)M^{p,r}_1(\xi_1),$$

and

$$f^{(i_1)}_{\Sigma^{(i)},(j_1,1)}(\xi_1,\xi_2) = \alpha^{(i,i_1)}(\xi_2)N^{p,r-1}_{j_1}(\xi_2)N^{p,r}_1(\xi_1).$$

Here the gluing data $\alpha^{(i,i_1)}$ and $\beta^{(i,i_1)}$ can be simply selected as

$$\alpha^{(i,i_1)}(\xi) = 1 \text{ and } \beta^{(i,i_1)}(\xi) = 0,$$

respectively, resulting in

$$f^{(i_1)}_{\Sigma^{(i)},(j_1,0)}(\xi_1,\xi_2) = N^{p,r+1}_{j_1}(\xi_2)M^{p,r}_0(\xi_1),$$

and

$$f^{(i_1)}_{\Sigma^{(i)},(j_1,1)}(\xi_1,\xi_2) = N^{p,r-1}_{j_1}(\xi_2)N^{p,r}_1(\xi_1).$$

Given a skeleton $\mathcal{M} = (\widehat{\Omega}, \mathcal{G}, \mathcal{T})$, the edge function spaces depend only on $\widehat{\Omega}$ and the edge gluing data $\mathcal{G}$ and are independent of the vertex data $\mathcal{T}$.

3.3. Vertex function space

The construction of the vertex function space $\mathcal{A}_{\mathbf{x}^{(i)}}$, for $i \in \mathcal{I}_\chi$, is derived from the planar construction developed in [20, 21]. There, for each vertex, six vertex functions are constructed as linear combinations of patch and modified edge functions in the vicinity of the considered vertex, where the corresponding scalar coefficients are determined by a C^2 interpolation problem at the vertex. As a consequence, the resulting vertex functions are not only C^1-smooth on the planar multi-patch domain, they are even C^2-smooth at the corresponding vertex. The imposed C^2-interpolation problem ensures a uniform construction of the vertex function space, such that its dimension is independent of the valence of the vertex and independent of the given patch parameterizations in the vicinity of the vertex. Here we follow this idea and adapt it appropriately. More precisely, we also generate six vertex functions for each vertex as linear combinations of patch and modified edge functions in the vicinity of the considered vertex. In contrast to the planar case, we construct the space by interpolation with respect to a projection of the local Taylor expansions onto the tangent plane at the vertex. Thus, we do not enforce a C^2-interpolation at the vertex with respect to the multi-patch surface domain Ω, which would require an underlying G^1-smooth multi-patch surface which additionally must be G^2-smooth at the vertex, and we would like to avoid this additional restriction.

Let us consider now the construction of the vertex function space $\widehat{\mathcal{A}}_{\mathbf{x}^{(i)}}$ in detail. For this purpose, we distinguish between the case of an inner vertex with $i \in \mathcal{I}_\chi^\circ$ and of a boundary vertex with $i \in \mathcal{I}_\chi^\Gamma$. We first consider an inner vertex with index $i \in \mathcal{I}_\chi^\circ$ and valence ν_i, with the sequence of surface patches and interface curves $\Sigma^{(i_1)}$, $\Omega^{(i_2)}$, $\Sigma^{(i_3)}$, …, $\Sigma^{(i_{2\nu_i-1})}$, $\Omega^{(i_{2\nu_i})}$ around the vertex in counterclockwise order in standard form, cf. Figure 3 (left) and Section 2.2.

In addition, let $\mathbf{F}_P^{(i_{2\ell})} \in (\mathcal{P}_2^2)^2$, $\ell = 1, \dots, \nu_i$, be the patch parameterizations, which are obtained by first rotating the Taylor expansions $\mathbf{F}_T^{(i_{2\ell})}$, $\ell = 1, \dots, \nu_i$, in such a way that their normal vectors at the vertex are parallel to the x_3-axis, and then by omitting the third component. Note that the resulting patch parameterizations $\mathbf{F}_P^{(i_{2\ell})}$, $\ell = 1, \dots, \nu_i$, locally represent the tangent plane at the vertex, which we denote by

$$\Omega_P = \cup_{\ell=1}^{2\nu_i} \overline{\Omega_P^{(i_{2\ell})}} \quad \text{with} \quad \Omega_P^{(i_{2\ell})} = \mathbf{F}_P^{(i_{2\ell})}((0,1)^2).$$

We further denote by $\mathbf{x}_P = (x_1^P, x_2^P)$ the global coordinates of Ω_P, by $\Sigma_P^{(i_{2\ell-1})}$, $\ell = 1, \dots, \nu_i$, the corresponding interface curves $\Sigma_P^{(i_{2\ell-1})}$, and by $\mathbf{x}_P^{(i)}$ the corresponding vertex $\mathbf{x}^{(i)}$ in Ω_P. Thanks to the performed rotation and projection, the gluing data is consistent with the planar patch parameterizations $\mathbf{F}_P^{(i_{2\ell})}$ if the skeleton was consistent.

For each interface curve $\Sigma_P^{(i_\ell)}$, $\ell = 1, 3, \dots, 2\nu_i - 1$, we define the vector functions

$$\mathbf{t}^{(i_\ell)}(\xi) = \partial_2 \mathbf{F}_P^{(i_{\ell-1})}(0, \xi) = \partial_1 \mathbf{F}_P^{(i_{\ell+1})}(\xi, 0)$$

and

$$\begin{aligned} \mathbf{d}^{(i_\ell)}(\xi) &= \tfrac{1}{\alpha^{(i_\ell, i_{\ell-1})}(\xi)} \left(\partial_1 \mathbf{F}_P^{(i_{\ell-1})}(0, \xi) + \beta^{(i_\ell, i_{\ell-1})}(\xi)\, \partial_2 \mathbf{F}_P^{(i_{\ell-1})}(0, \xi) \right) \\ &= -\tfrac{1}{\alpha^{(i_\ell, i_{\ell+1})}(\xi)} \left(\partial_2 \mathbf{F}_P^{(i_{\ell+1})}(\xi, 0) + \beta^{(i_\ell, i_{\ell+1})}(\xi)\, \partial_1 \mathbf{F}_P^{(i_{\ell+1})}(\xi, 0) \right). \end{aligned}$$

For a vector $\mathbf{a} = \begin{bmatrix} a_{0,0} & a_{1,0} & a_{0,1} & a_{2,0} & a_{1,1} & a_{0,2} \end{bmatrix} \in \mathbb{R}^6$, we define for each patch $\Omega_P^{(i_\ell)}$, $\ell \in \{2, 4 \ldots, 2\nu_i\}$, the function

$$f^{(i_\ell)}_{\mathbf{x}^{(i)},\mathbf{a}}(\xi_1, \xi_2) = g^{(i_{\ell-1},i_\ell)}_{\mathbf{x}^{(i)},\mathbf{a}}(\xi_1, \xi_2) + g^{(i_{\ell+1},i_\ell)}_{\mathbf{x}^{(i)},\mathbf{a}}(\xi_1, \xi_2) - g^{(i_\ell)}_{\mathbf{x}^{(i)},\mathbf{a}}(\xi_1, \xi_2)$$

with the single functions

$$\begin{aligned} g^{(i_{\ell+1},i_\ell)}_{\mathbf{x}^{(i)},\mathbf{a}}(\xi_1, \xi_2) = &\sum_{j=0}^{2} d^{(i_{\ell+1},i_\ell)}_{\mathbf{a},(0,j)} \left(M_j^{p,r+1}(\xi_2) M_0^{p,r}(\xi_1) - \beta^{(i_{\ell+1},i_\ell)}(\xi_2) (M_j^{p,r+1})'(\xi_2) M_1^{p,r}(\xi_1) \right) \\ &+ \sum_{j=0}^{1} d^{(i_{\ell+1},i_\ell)}_{\mathbf{a},(1,j)} \alpha^{(i_{\ell+1},i_\ell)}(\xi_2) M_j^{p-1,r}(\xi_2) M_1^{p,r}(\xi_1), \end{aligned}$$

$$\begin{aligned} g^{(i_{\ell-1},i_\ell)}_{\mathbf{x}^{(i)},\mathbf{a}}(\xi_1, \xi_2) = &\sum_{j=0}^{2} d^{(i_{\ell-1},i_\ell)}_{\mathbf{a},(0,j)} \left(M_j^{p,r+1}(\xi_1) M_0^{p,r}(\xi_2) - \beta^{(i_{\ell-1},i_\ell)}(\xi_1) (M_j^{p,r+1})'(\xi_1) M_1^{p,r}(\xi_2) \right) \\ &- \sum_{j=0}^{1} d^{(i_{\ell-1},i_\ell)}_{\mathbf{a},(1,j)} \alpha^{(i_{\ell-1},i_\ell)}(\xi_1) M_j^{p-1,r}(\xi_1) M_1^{p,r}(\xi_2), \end{aligned}$$

and

$$g^{(i_\ell)}_{\mathbf{x}^{(i)},\mathbf{a}}(\xi_1, \xi_2) = \sum_{j_1=0}^{1} \sum_{j_2=0}^{1} d^{(i_\ell)}_{\mathbf{a},(j_1,j_2)} M_{j_1}^{p,r}(\xi_1) M_{j_2}^{p,r}(\xi_2),$$

where the corresponding coefficients are given by

$$d^{(i_m,i_\ell)}_{\mathbf{a},(0,0)} = a_{0,0},\ d^{(i_m,i_\ell)}_{\mathbf{a},0,1} = \mathbf{b_a}\ \mathbf{t}^{(i_m)}(0),\ d^{(i_m,i_\ell)}_{\mathbf{a},0,2} = (\mathbf{t}^{(i_m)}(0))^T\ H_{\mathbf{a}}\ \mathbf{t}^{(i_m)}(0) + \mathbf{b_a}\ (\mathbf{t}^{(i_m)})'(0),$$

$$d^{(i_m,i_\ell)}_{\mathbf{a},(1,0)} = \mathbf{b_a}\ \mathbf{d}^{(i_m)}(0),\ d^{(i_m,i_\ell)}_{\mathbf{a},(1,1)} = (\mathbf{t}^{(i_m)}(0))^T\ H_{\mathbf{a}}\ \mathbf{d}^{(i_m)}(0) + \mathbf{b_a}\ (\mathbf{d}^{(i_m)})'(0),$$

for $m = \ell - 1, \ell + 1$, and

$$d^{(i_\ell)}_{\mathbf{a},(0,0)} = a_{0,0},\ d^{(i_\ell)}_{\mathbf{a},(1,0)} = \mathbf{b_a}\ \mathbf{t}^{(i_{\ell-1})}(0),\ d^{(i_\ell)}_{\mathbf{a},(0,1)} = \mathbf{b_a}\ \mathbf{t}^{(i_{\ell+1})}(0)$$

$$d^{(i_\ell)}_{\mathbf{a},(1,1)} = (\mathbf{t}^{(i_{\ell-1})}(0))^T\ H_{\mathbf{a}}\ \mathbf{t}^{(i_{\ell+1})}(0) + \mathbf{b_a}\ \partial_1\partial_2 \mathbf{F}_P^{(i_\ell)}(0,0),$$

where $\mathbf{b_a}$ is further the vector $\mathbf{b_a} = \begin{bmatrix} a_{1,0} & a_{0,1} \end{bmatrix}$ and $H_{\mathbf{a}}$ is the matrix

$$H_{\mathbf{a}} = \begin{bmatrix} a_{2,0} & a_{1,1} \\ a_{1,1} & a_{0,2} \end{bmatrix}.$$

Moreover, we consider the six vectors

$$\mathbf{a}_{(0,0)} = (1,0,0,0,0,0),\ \mathbf{a}_{(1,0)} = (0,1,0,0,0,0),\ \mathbf{a}_{(0,1)} = (0,0,1,0,0,0),$$

$$\mathbf{a}_{(2,0)} = (0,0,0,1,0,0),\ \mathbf{a}_{(1,1)} = (0,0,0,0,1,0),\ \mathbf{a}_{(0,2)} = (0,0,0,0,0,1),$$

and specify the factor

$$\sigma = \left(\frac{h}{p\,\nu_i} \sum_{\ell=1}^{\nu} \|\nabla \mathbf{F}_P^{(i_{2\ell})}(0,0)\| \right)^{-1},$$

which will be used to uniformly scale the vertex functions with respect to the L^∞-norm.

The vertex function space $\widehat{\mathcal{A}}_{\mathbf{x}^{(i)}}$ is defined as

$$\widehat{\mathcal{A}}_{\mathbf{x}^{(i)}} = \operatorname{span}\{\widehat{\phi}_{\mathbf{x}^{(i)},(j_1,j_2)} :\ 0 \le j_1, j_2 \le 2,\ j_1 + j_2 \le 2\}, \tag{13}$$

where

$$\widehat{\phi}_{\mathbf{x}^{(i)},(j_1,j_2)}(\boldsymbol{\xi}) = \begin{cases} \sigma^{j_1+j_2} f^{(i_\ell)}_{\mathbf{x}^{(i)},\mathbf{a}_{(j_1,j_2)}}(\boldsymbol{\xi}) & \text{if } \boldsymbol{\xi} \in \widehat{\Omega}^{(i_\ell)},\ \ell = 2, 4, \ldots, 2\nu_i, \\ 0 & \text{otherwise.} \end{cases} \tag{14}$$

Let now $\mathbf{x}^{(i)}$, $i \in \mathcal{I}_\chi^\Gamma$, be a boundary vertex of patch valence ν_i with the sequence of surface patches and interface/boundary curves $\Sigma^{(i_1)}$, $\Omega^{(i_2)}$, $\Sigma^{(i_3)}$, …, $\Omega^{(i_{2\nu_i})}$, $\Sigma^{(i_{2\nu_i+1})}$ around the vertex $\mathbf{x}^{(i)}$ in counterclockwise order, where $\Sigma^{(i_1)}$ and $\Sigma^{(i_{2\nu_i+1})}$ represent the boundary curves, given in standard form, cf. Figure 3 (right) and Section 2.2. The construction of the functions $\widehat{\phi}_{\mathbf{x}^{(i)},(j_1,j_2)}$, $0 \le j_1, j_2 \le 2$ with $j_1 + j_2 \le 2$ works analogously as for the case of an inner vertex via (14) and (13), respectively, by selecting the gluing data $\alpha^{(i_1,i_2)}$, $\beta^{(i_1,i_2)}$ and $\alpha^{(i_{2\nu_i+1},i_{2\nu_i})}$, $\beta^{(i_{2\nu_i+1},i_{2\nu_i})}$ of the boundary curves as

$$\alpha^{(i_1,i_2)}(\xi) = 1,\ \beta^{(i_1,i_2)}(\xi) = 0,$$

and

$$\alpha^{(i_{2\nu_i+1},i_{2\nu_i})}(\xi) = 1,\ \beta^{(i_{2\nu_i+1},i_{2\nu_i})}(\xi) = 0,$$

respectively.

Remark 1. The functions $\widehat{\phi}_{\mathbf{x}^{(i)},(j_1,j_2)}$ yield functions $\phi_{\mathbf{x}_P^{(i)},(j_1,j_2)}$ on Ω_P through

$$\phi_{\mathbf{x}_P^{(i)},(j_1,j_2)} = \widehat{\phi}_{\mathbf{x}^{(i)},(j_1,j_2)} \circ \mathbf{F}_P^{-1}.$$

By construction the functions are C^1-smooth on Ω_P and C^2-smooth at the vertex $\mathbf{x}_P^{(i)}$. The C^1-continuity on Ω_P is a direct consequence of the fact that a function $\phi_{\mathbf{x}_P^{(i)},(j_1,j_2)}$ simplifies in the vicinity of an interface curve $\Sigma_P^{(i_\ell)}$, $\ell = 1, 3, \ldots, 2\nu_i - 1$, on the patch $\Omega_P^{(i_{\ell-1})}$ to $g^{(i_\ell,i_{\ell-1})}_{\mathbf{x}^{(i)},\mathbf{a}_{(j_1,j_2)}} \circ \left(\mathbf{F}_P^{(i_{\ell-1})}\right)^{-1}$ and on the patch $\Omega_P^{(i_{\ell+1})}$ to $g^{(i_\ell,i_{\ell+1})}_{\mathbf{x}^{(i)},\mathbf{a}_{(j_1,j_2)}} \circ \left(\mathbf{F}_P^{(i_{\ell+1})}\right)^{-1}$, where the simplified function at the interface curve $\Sigma_P^{(i_\ell)}$ represents a linear combination of modified edge functions which is C^1-smooth across the interface curve $\Sigma_P^{(i_\ell)}$, since the functions $g^{(i_\ell,i_{\ell-1})}_{\mathbf{x}^{(i)},\mathbf{a}_{(j_1,j_2)}}$ and $g^{(i_\ell,i_{\ell+1})}_{\mathbf{x}^{(i)},\mathbf{a}_{(j_1,j_2)}}$ fulfill the C^1-continuity conditions (9) and (11). The C^2-continuity at the vertex $\mathbf{x}_P^{(i)}$ is obtained by interpolating the C^2 data given by the vectors $\mathbf{a}_{(j_1,j_2)}$, $0 \le j_1, j_2 \le 2$ with $j_1 + j_2 \le 2$, which directly implies that

$$\partial^{m_1}_{x_1^P} \partial^{m_2}_{x_2^P} \left(\phi_{\mathbf{x}_T^{(i)},(j_1,j_2)} \right) (\mathbf{x}_P^{(i)}) = \sigma^{j_1+j_2} \delta^{m_1}_{j_1}\ \delta^{m_2}_{j_2}$$

for $0 \le m_1, m_2 \le 2$ with $m_1 + m_2 \le 2$, compare also [20, 21].

3.4. The C^1-smooth space $\mathcal{A}$

In the previous subsections we defined patch, edge and vertex spaces on the multi-patch parameter domain $\widehat{\Omega}$. By construction, we have the following.

Lemma 1. *Let Λ be the set of all patch function spaces $\widehat{\mathcal{A}}_{\Omega^{(i)}}$, $i \in \mathcal{I}_\Omega$, edge function spaces $\widehat{\mathcal{A}}_{\Sigma^{(i)}}$, $i \in \mathcal{I}_\Sigma$, and vertex function spaces $\widehat{\mathcal{A}}_{\mathbf{x}^{(i)}}$, $i \in \mathcal{I}_\chi$. For any two different spaces $\widehat{\mathcal{A}}_1, \widehat{\mathcal{A}}_2 \in \Lambda$, it holds that*

$$\widehat{\mathcal{A}}_1 \cap \widehat{\mathcal{A}}_2 = \{0\}.$$

Due to Lemma 1 we can define the space $\widehat{\mathcal{A}}$ as the direct sum of the local spaces

$$\widehat{\mathcal{A}} = \left(\bigoplus_{i\in\mathcal{I}_\Omega} \widehat{\mathcal{A}}_{\Omega^{(i)}}\right) \oplus \left(\bigoplus_{i\in\mathcal{I}_\Sigma} \widehat{\mathcal{A}}_{\Sigma^{(i)}}\right) \oplus \left(\bigoplus_{i\in\mathcal{I}_\chi} \widehat{\mathcal{A}}_{\mathbf{x}^{(i)}}\right) \subset \mathcal{S}, \tag{15}$$

where $\mathcal{S}$ is the C^0-smooth multi-patch spline space on the parameter domain $\widehat{\Omega}$. Given a multi-patch parameterization $\mathbf{F} \in (\widehat{\mathcal{A}})^3$ we can define the isogeometric space

$$\mathcal{A} = \left\{\varphi \in C^0(\Omega) \ : \ \varphi \circ \mathbf{F} \in \widehat{\mathcal{A}}\right\}.$$

Similarly, we can define the subspaces $\mathcal{A}_{\Omega^{(i)}}$, $\mathcal{A}_{\Sigma^{(i)}}$ and $\mathcal{A}_{\mathbf{x}^{(i)}}$ that yield the direct sum as in (12) and their basis functions $\phi_{\Omega^{(i)},\mathbf{j}}$, $\phi_{\Sigma^{(i)},\mathbf{j}}$ and $\phi_{\mathbf{x}^{(i)},\mathbf{j}}$, respectively, through the mapping $\mathbf{F}$. By construction we have that all patch functions are C^1-smooth on Ω.

Lemma 2. *Let $i \in \mathcal{I}_\Omega$. It holds that*

$$\mathcal{A}_{\Omega^{(i)}} \subset \mathcal{V}^1.$$

Proof. All functions $\phi_{\Omega^{(i)},\mathbf{j}}$, $\mathbf{j} \in \{2,\dots,n-3\}^2$, fulfill that $\operatorname{supp}\left(\phi_{\Omega^{(i)},\mathbf{j}}\right) \subset \Omega^{(i)}$ and that $\phi_{\Omega^{(i)},\mathbf{j}}(\mathbf{x}) = \nabla\phi_{\Omega^{(i)},\mathbf{j}}(\mathbf{x}) = 0$ for $\mathbf{x} \in \partial\Omega^{(i)}$, which trivially implies that $\mathcal{A}_{\Omega^{(i)}} \subset \mathcal{V}^1$. □

Similarly, all edge functions are C^1-smooth.

Lemma 3. *Let $i \in \mathcal{I}_\Sigma$. We have that*

$$\mathcal{A}_{\Sigma^{(i)}} \subset \mathcal{V}^1.$$

Proof. In case of an interface curve $\Sigma^{(i)}$, that is, $i \in \mathcal{I}_\Sigma^\circ$, all functions $\phi_{\Sigma^{(i)},(j_1,j_2)}$, $j_1 = 3-j_2,\dots,n_{j_2}-4+j_2$, $j_2 = 0,1$, satisfy that $\operatorname{supp}\left(\phi_{\Sigma^{(i)},\mathbf{j}}\right) \subset \overline{\Omega^{(i_1)}} \cup \overline{\Omega^{(i_1)}}$ and that $\phi_{\Sigma^{(i)},\mathbf{j}}(\mathbf{x}) = \nabla\phi_{\Sigma^{(i)},\mathbf{j}}(\mathbf{x}) = 0$ for $\mathbf{x} \in \partial\left(\overline{\Omega^{(i_1)}} \cup \overline{\Omega^{(i_1)}}\right)$. In addition, their associated spline functions $f^{(i_1)} = \phi_{\Sigma^{(i)},\mathbf{j}} \circ \mathbf{F}^{(i_1)} = f^{(i_1)}_{\Sigma^{(i)},\mathbf{j}}$ and $f^{(i_2)} = \varphi \circ \mathbf{F}^{(i_2)} = f^{(i_2)}_{\Sigma^{(i)},\mathbf{j}}$ fulfill the C^1-continuity conditions (9) and (11) across the interface curve $\Sigma^{(i)}$, which further leads to $\mathcal{A}_{\Sigma^{(i)}} \subset \mathcal{V}^1$.

In case of a boundary curve $\Sigma^{(i)}$, that is, $i \in \mathcal{I}_\Sigma^\Gamma$, we trivially obtain that $\mathcal{A}_{\Sigma^{(i)}} \subset \mathcal{V}^1$, since for all functions $\phi_{\Sigma^{(i)},(j_1,j_2)}$, $j_1 = 3-j_2,\dots,n_{j_2}-4+j_2$, $j_2 = 0,1$, we have that that $\operatorname{supp}\left(\phi_{\Sigma^{(i)},\mathbf{j}}\right) \subset \overline{\Omega^{(i)}}$ and that $\phi_{\Sigma^{(i)},\mathbf{j}}(\mathbf{x}) = \nabla\phi_{\Sigma^{(i)},\mathbf{j}}(\mathbf{x}) = 0$ for $\mathbf{x} \in \partial\Omega^{(i)} \setminus \Sigma^{(i)}$. □

Similar to the planar case, the vertex functions are C^1-smooth, now on the multi-patch surface domain Ω, but in contrast to the planar construction as in [20, 21] in general not additionally C^2-smooth at the corresponding vertex $\mathbf{x}^{(i)}$.

Lemma 4. *Let $i \in \mathcal{I}_\chi$. It holds that*

$$\mathcal{A}_{\mathbf{x}^{(i)}} \subset \mathcal{V}^1.$$

Proof. Let us consider first the case of an inner vertex $\mathbf{x}^{(i)}$, that is, $i \in \mathcal{I}_\chi^\circ$. Since all six functions $\phi_{\mathbf{x}^{(i)},(j_1,j_2)}$, $0 \leq j_1, j_2 \leq 2$ with $j_1 + j_2 \leq 2$, are C^1-smooth across the interface curves $\Sigma^{(i_\ell)}$, $\ell = 1, 3, \ldots, 2\nu_i - 1$, and further fulfill that $\operatorname{supp}\left(\phi_{\mathbf{x}^{(i)},(j_1,j_2)}\right) \subset \cup_{\ell=1}^{\nu_i} \overline{\Omega^{(i_{2\ell})}}$ and that $\phi_{\mathbf{x}^{(i)},(j_1,j_2)}(\mathbf{x}) = \nabla\phi_{\mathbf{x}^{(i)},(j_1,j_2)}(\mathbf{x}) = 0$ for $\mathbf{x} \in \partial\left(\cup_{\ell=1}^{\nu_i} \overline{\Omega^{(i_{2\ell})}}\right)$, we directly obtain that $\mathcal{A}_{\mathbf{x}^{(i)}} \subset \mathcal{V}^1$.

Similarly, we also obtain $\mathcal{A}_{\mathbf{x}^{(i)}} \subset \mathcal{V}^1$ for the case of a boundary vertex $\mathbf{x}^{(i)}$, that is, $i \in \mathcal{I}_\chi^\Gamma$, because all six functions $\phi_{\mathbf{x}^{(i)},(j_1,j_2)}$, $0 \leq j_1, j_2 \leq 2$ with $j_1 + j_2 \leq 2$, are C^1-smooth across the interface curves $\Sigma^{(i_\ell)}$, $\ell = 3, 5, \ldots, 2\nu_i - 1$, are only supported in $\cup_{\ell=1}^{\nu_i} \overline{\Omega^{(i_{2\ell})}}$, and possess vanishing values and gradients at all interface and boundary curves except at the interface and boundary curves $\Sigma^{(i_\ell)}$, $\ell = 1, 3, \ldots, 2\nu_i + 1$. □

Summarizing the above we obtain:

Theorem 1. *The space $\mathcal{A}$, given by the direct sum (12), is a subspace of the C^1-smooth space $\mathcal{V}^1$, i.e $\mathcal{A} \subset \mathcal{V}^1$. Moreover, the patch functions $\phi^{(i)}_{\Omega^{(i)},\mathbf{j}}$, $\mathbf{j} \in \{2, \ldots, n-3\}^2$, $i \in \mathcal{I}_\Omega$, the edge functions $\phi_{\Sigma^{(i)},(j_1,j_2)}$, $j_1 = 3 - j_2, \ldots, n_{j_2} - 4 + j_2$, $j_2 = 0, 1$, $i \in \mathcal{I}_\Sigma$, and the vertex functions $\phi_{\mathbf{x}^{(i)},(j_1,j_2)}$, $0 \leq j_1, j_2 \leq 2$ and $j_1 + j_2 \leq 2$, $i \in \mathcal{I}_\chi$, form a basis of the space $\mathcal{A}$, and the dimension of $\mathcal{A}$ is equal to*

$$\dim \mathcal{A} = \sum_{i \in \mathcal{I}_\Omega} \dim \mathcal{A}_{\Omega^{(i)}} + \sum_{i \in \mathcal{I}_\Sigma} \dim \mathcal{A}_{\Sigma^{(i)}} + \sum_{i \in \mathcal{I}_\chi} \dim \mathcal{A}_{\mathbf{x}^{(i)}}$$

with

$$\dim \mathcal{A}_{\Omega^{(i)}} = \left((p-r)(k-1) + p - 3\right)^2,$$
$$\dim \mathcal{A}_{\Omega^{(i)}} = (2(p-r-1)(k-1) + p - 9)$$

and

$$\dim \mathcal{A}_{\Omega^{(i)}} = 6.$$

Proof. $\mathcal{A} \subset \mathcal{V}^1$ is a direct consequence of Lemma 2, 3 and 4. Since the the patch functions $\phi^{(i)}_{\Omega^{(i)},\mathbf{j}}$, $\mathbf{j} \in \{2, \ldots, n-3\}^2$, the edge functions $\phi_{\Sigma^{(i)},(j_1,j_2)}$, $j_1 = 3 - j_2, \ldots, n_{j_2} - 4 + j_2$, $j_2 = 0, 1$, and the vertex functions $\phi_{\mathbf{x}^{(i)},(j_1,j_2)}$, $0 \leq j_1, j_2 \leq 2$ with $j_1 + j_2 \leq 2$, are linearly independent by definition and/or construction for the corresponding patch function space $\mathcal{A}_{\Omega^{(i)}}$, $i \in \mathcal{I}_\Omega$, edge function space $\mathcal{A}_{\Sigma^{(i)}}$, $i \in \mathcal{I}_\Sigma$, and vertex function space $\mathcal{A}_{\mathbf{x}^{(i)}}$, $i \in \mathcal{I}_\chi$, respectively, and due to direct sum (12), all patch, edge and vertex functions form together a basis of the space $\mathcal{A}$. This further directly implies the dimensions of the individual patch, edge and vertex function spaces and hence of the C^1-smooth space $\mathcal{A}$. □

4. Design of AS-G^1 multi-patch surfaces

We present a novel methodology for the construction of AS-G^1 multi-patch surfaces. For this purpose, we first introduce a general framework to generate AS-G^1 multi-patch surfaces and then describe two specific design methods which are based on this methodology.

4.1. General framework for the construction of AS-G^1 multi-patch surfaces

We consider the following problem: Given a G^1-smooth but non-AS-G^1 multi-patch surface $\mathbf{R}$ over the multi-patch parameter domain $\widehat{\Omega}$, we aim to generate an AS-G^1 multi-patch surface $\mathbf{F}$ over the same parameter domain $\widehat{\Omega}$, with suitable gluing data $\mathcal{G}$ and vertex data $\mathcal{T}$, such that $\mathbf{F} \in (\widehat{\mathcal{A}})^3$, where $\widehat{\mathcal{A}}$ is constructed from the AS-G^1 skeleton $\mathcal{M} = (\widehat{\Omega}, \mathcal{G}, \mathcal{T})$, which approximates the multi-patch surface $\mathbf{R}$ as good as possible. Our proposed strategy for solving the stated problem consists of two main steps:

Step 1: Computation of an AS-G^1 skeleton from a multi-patch template parameterization. Given the parameter domain $\widehat{\Omega}$ of $\mathbf{R}$ we choose an AS-G^1 multi-patch parameterization $\widetilde{\mathbf{F}}$ over $\widehat{\Omega}$, which will play the role of a template parameterization in the L^2-projection procedure in Step 2. In case of an open planarizable surface $\mathbf{R}$, a planar AS-G^1 multi-patch template can be used, for which several design methods such as the techniques developed in [19, 20] exist (compare also Section 4.2.1). In case of a closed surface which is topologically equivalent to a sphere, a closed AS-G^1 multi-patch surface as the one in Example 6, first constructed in [19, Example 5], could be employed. From such a multi-patch template $\widetilde{\mathbf{F}}$ we extract the skeleton $\mathcal{M}$.

Step 2: Construction of the AS-G^1 multi-patch surface via L^2-projection. Let $\widetilde{\mathbf{F}}$ be the template from Step 1 and let $\mathcal{M}$ be its skeleton. We denote by $\widetilde{\Omega}$ the surface domain obtained from $\widetilde{\mathbf{F}}$, i.e., $\widetilde{\Omega} = \widetilde{\mathbf{F}}(\widehat{\Omega})$. Following the construction proposed in Section 3, we generate the space $\widehat{\mathcal{A}}$ of degree $\mathbf{p} = (p, p)$, regularity $\mathbf{r} = (r, r)$ and mesh size h from the skeleton $\mathcal{M}$, such that $\widetilde{\mathbf{F}} \in (\widehat{\mathcal{A}})^d$, with $d \in \{2, 3\}$. Let $\{\phi_j\}_{j\in\mathcal{J}}$, $\mathcal{J} = \{1, \dots \dim \mathcal{A}\}$, be the basis of the corresponding isogeometric spline space $\mathcal{A}$ over $\widetilde{\Omega}$. We now construct the desired AS-G^1 multi-patch surface $\mathbf{F}$ through finding a mapping $\mathbf{U}$, with $\mathbf{U} \in (\mathcal{A})^3$, such that

$$\mathbf{F} = \mathbf{U} \circ \widetilde{\mathbf{F}},$$

with

$$\mathbf{U}(\mathbf{x}) = \sum_{j\in\mathcal{J}} \mathbf{d}_j \phi_j(\mathbf{x}), \quad \mathbf{d}_j = \begin{bmatrix} d_{j,1} & d_{j,2} & d_{j,3} \end{bmatrix}^T \in \mathbb{R}^3, \quad \mathbf{x} \in \widetilde{\Omega}.$$

Thus we determine the unknown coefficients $\mathbf{d}_j$ via L^2-projection by minimizing the objective function

$$\left\| \mathbf{U} - \mathbf{R} \circ \widetilde{\mathbf{F}}^{-1} \right\|^2_{L^2(\widetilde{\Omega})},$$

which results in minimizing the error for each component via

$$\sum_{i\in\mathcal{I}_\Omega} \int_{[0,1]^2} \left(F_\ell^{(i)}(\boldsymbol{\xi}) - R_\ell^{(i)}(\boldsymbol{\xi}) \right)^2 \widetilde{g}^{(i)}(\boldsymbol{\xi}) d\boldsymbol{\xi}, \quad \ell = 1, 2, 3,$$

where $\widetilde{g}^{(i)}$ is the square root of the determinant of the coefficients of the first fundamental form of the surface patch parameterization $\widetilde{\mathbf{F}}^{(i)}$, cf. Section 2.3. We denote by $R_\ell^{(i)}$ the ℓ-th component of the i-th patch of $\mathbf{R}$. The mappings $\mathbf{R}$, $\widetilde{\mathbf{F}}$ and $\mathbf{U}$ are visualized in Figure 4.

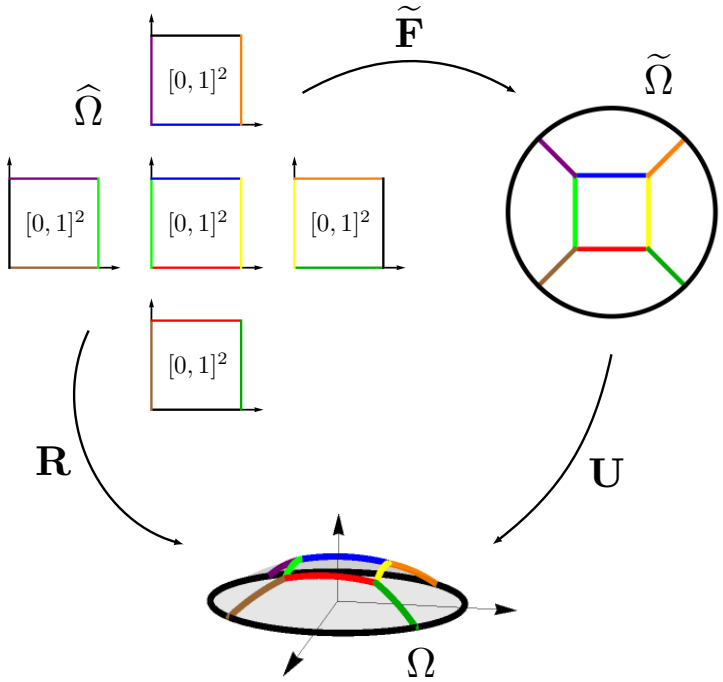

Figure 4: A schematic overview of the mappings involved in the construction framework. The parameter domain $\widehat{\Omega}$ is formed by five unit squares, where the equivalence relation is visualized through colors, i.e., each point on a colored edge corresponds to a point on another edge of the same color. The corresponding interfaces are shown in the same color, both on the template domain $\widetilde{\Omega}$ and on the target domain Ω. Boundary edges are shown as black lines.

In case that the resulting AS-G^1 multi-patch surface $\mathbf{F}$ does not approximate the initial surface $\mathbf{R}$ as good as wanted, we can just perform h- or p-refinement for the C^1-smooth spline space $\widehat{\mathcal{A}}$ to improve the approximation.

Remark 2. The general framework for the construction of AS-G^1 multi-patch surfaces is not limited to G^1-smooth multi-patch surfaces, but can be also directly applied to any (approximately) smooth surface which can be approximated as a first step by a G^1-smooth multi-patch surface. A first such possible example is a trimmed surface which can be represented after an untrimming procedure, see e.g. [32], by a multi-patch surface, compare also Section 4.2.2. A subdivision surface is another possible example, see e.g. [30], but this case will not be further studied in this work.

4.2. Methods for the design of AS-G^1 multi-patch surfaces

We describe two specific methods for the construction of AS-G^1 multi-patch surfaces which are based on the general framework introduced in the previous subsection.

4.2.1. AS-G^1 multi-patch surfaces for graph surfaces

We present a technique to generate an AS-G^1 multi-patch surface by approximating a graph of a function given over a planar multi-patch domain. Let $\widetilde{\Omega}$ be the planar multi-patch domain, and let $\widetilde{\mathbf{F}}$ with the single geometry mappings $\widetilde{\mathbf{F}}^{(i)}$, $i \in \mathcal{I}_\Omega$, be a planar AS-G^1 multi-patch parameterization which represents the planar multi-patch domain $\widetilde{\Omega}$. Note that such a planar AS-G^1 multi-patch geometry $\widetilde{\mathbf{F}}$ can be constructed e.g. by means of the method [19]. We consider a smooth function $z : \widetilde{\Omega} \to \mathbb{R}$, which defines via

$$\mathbf{R}(\widetilde{\mathbf{x}}) = \begin{bmatrix} \widetilde{\mathbf{x}} & z(\widetilde{\mathbf{x}}) \end{bmatrix}^T, \quad \widetilde{\mathbf{x}} = (\widetilde{x}_1, \widetilde{x}_2) \in \widetilde{\Omega},$$

a surface in $\mathbb{R}^3$, the so-called graph surface of the function z over the planar multi-patch domain $\widetilde{\Omega}$. The resulting graph surface $\mathbf{R}$ represents also a multi-patch surface via the single surface patch parameterizations $\mathbf{R}^{(i)}$, $i \in \mathcal{I}_\Omega$, which are given by

$$\mathbf{R}^{(i)}(\boldsymbol{\xi}) = \begin{bmatrix} \widetilde{\mathbf{F}}^{(i)}(\boldsymbol{\xi}) & \left(z \circ \widetilde{\mathbf{F}}^{(i)}\right)(\boldsymbol{\xi}) \end{bmatrix}^T.$$

The goal is now to find an AS-G^1 multi-patch surface $\mathbf{F}$ with surface patch parameterizations $\mathbf{F}^{(i)}$, $i \in \mathcal{I}_\Omega$, which approximates the multi-patch surface $\mathbf{R}$ as good as possible. For this purpose, we first generate the C^1-smooth isogeometric spline space $\mathcal{A}$ over the planar multi-patch parameterization $\widetilde{\mathbf{F}}$ for some degree $\mathbf{p} = (p, p)$, regularity $\mathbf{r} = (r, r)$ and mesh size h by using the method [21], or equivalently by following the construction from Section 3 by just extending the planar multi-patch parameterization $\widetilde{\mathbf{F}}$ to a third coordinate which is set to be zero. We denote again by $\{\phi_j\}_{j \in \mathcal{J}}$ the basis of $\mathcal{A}$. As a slight modification to the general framework from the previous subsection, we have now just to approximate the third coordinate function of the multi-patch surface $\mathbf{R}$, since the first two coordinates already satisfy by definition the AS-G^1 condition (5). That is, we build the AS-G^1 multi-patch surface $\mathbf{F}$ by constructing the single surface patch parameterizations $\mathbf{F}^{(i)}$, $i \in \mathcal{I}_\Omega$, as

$$\mathbf{F}^{(i)}(\boldsymbol{\xi}) = \begin{bmatrix} F_1^{(i)}(\boldsymbol{\xi}) & F_2^{(i)}(\boldsymbol{\xi}) & F_3^{(i)}(\boldsymbol{\xi}) \end{bmatrix} = \begin{bmatrix} \widetilde{\mathbf{F}}^{(i)}(\boldsymbol{\xi}) & \left(u \circ \widetilde{\mathbf{F}}^{(i)}\right)(\boldsymbol{\xi}) \end{bmatrix}$$

with

$$u(\mathbf{x}) = \sum_{j \in \mathcal{J}} d_j \phi_j(\mathbf{x}), \quad d_j \in \mathbb{R}, \quad \mathbf{x} \in \widetilde{\Omega},$$

by selecting the unknown coefficients d_j via minimizing

$$\sum_{i \in \mathcal{I}_\Omega} \int_{[0,1]^2} \left(F_3^{(i)}(\boldsymbol{\xi}) - R_3^{(i)}(\boldsymbol{\xi})\right)^2 \widetilde{g}^{(i)}(\boldsymbol{\xi}) d\boldsymbol{\xi},$$

where $\widetilde{g}^{(i)}$ is as in the general framework above the square root of the determinant of the coefficients of the first fundamental form of the patch parameterization $\widetilde{\mathbf{F}}^{(i)}$, cf. Section 2.3.

In the following example, we use the presented method to construct AS-G^1 multi-patch surfaces which approximate a portion of a sphere.

Example 1. We construct the three AS-G^1 multi-patch surfaces $\mathbf{F}_\ell$, $\ell = 1, 2, 3$, shown in Figure 5 (second row, from left to right), from the three planar multi-patch parameterizations $\widetilde{\mathbf{F}}_\ell$, $\ell = 1, 2, 3$, given in Figure 5 (first row, from left to right), by approximating the function

$$z(\widetilde{x}_1, \widetilde{x}_2) = \sqrt{6 - \widetilde{x}_1^2 - \widetilde{x}_2^2}.$$

While the four-patch parameterization $\widetilde{\mathbf{F}}_1$ (Figure 5, first row, left) and the six-patch parameterization $\widetilde{\mathbf{F}}_2$ (Figure 5, first row, middle) are bilinearly parameterized and hence trivially AS-G^1, the five-patch parameterization $\widetilde{\mathbf{F}}_3$ (Figure 5, first row, right) is an AS-G^1 five patch geometry constructed by the method [19], which approximates a disk and consists of patch parameterizations $\widetilde{\mathbf{F}}_\ell^{(i)} \in (\mathcal{S}_h^{\mathbf{p},\mathbf{r}})^2$ with $\mathbf{p} = (3, 3)$, $\mathbf{r} = (1, 1)$ and $h = \frac{1}{3}$. All three resulting AS-G^1 multi-patch surfaces $\mathbf{F}_\ell$, $\ell = 1, 2, 3$, approximate then a portion of a sphere and consist of surface patch parameterizations $\mathbf{F}_\ell^{(i)}$ belonging to the space $(\mathcal{S}_h^{\mathbf{p},\mathbf{r}})^3$ with $\mathbf{p} = (3, 3)$, $\mathbf{r} = (1, 1)$ and $h = \frac{1}{3}$, see Figure 5 (second row). In Example 5, the constructed AS-G^1 multi-patch surfaces $\mathbf{F}_\ell$, $\ell = 1, 2, 3$, will be employed to solve the biharmonic equation over them.

4.2.2. AS-G^1 multi-patch surfaces for trimmed surfaces

We can use the general framework from Section 4.1 to approximate a trimmed smooth surface by an AS-G^1 multi-patch surface. Let $\mathbf{S}_t$ be a trimmed smooth surface which is defined via a trimmed parameter domain D_t and a smooth tensor-product spline surface $\mathbf{S}$ with parameter domain $D \supset D_t$. By using e.g. the untrimming technique [32], we can represent the trimmed smooth surface $\mathbf{S}_t$ by a smooth multi-patch surface $\mathbf{R}$ consisting of single surface patch parameterizations $\mathbf{R}^{(i)} \in \left(\mathcal{S}_{h'}^{\mathbf{p}',\mathbf{r}'}\right)^3$, $i \in \mathcal{I}_\Omega$. This is done by first describing the trimmed parameter domain D_t by a planar multi-patch parameterization, and then by using this parameterization to construct the smooth multi-patch surface $\mathbf{R}$. Afterwards, by directly applying the general framework from Section 4.1, we can approximate the multi-patch surface $\mathbf{R}$ by an AS-G^1 multi-patch surface $\mathbf{F}$ consisting of surface patch parameterizations $\mathbf{F}^{(i)} \in (\mathcal{S}_h^{\mathbf{p},\mathbf{r}})^3$, $i \in \mathcal{I}_\Omega$, with some degree $\mathbf{p} = (p, p)$, regularity $\mathbf{r} = (r, r)$, mesh size h and with the same index set $\mathcal{I}_\Omega$ as for the multi-patch surface $\mathbf{R}$.

In case that the surface $\mathbf{S}$ possesses a polynomial representation, the construction of the AS-G^1 multi-patch surface $\mathbf{F}$ can be simplified as follows. We generate first again a planar multi-patch parameterization of the trimmed parameter domain D_t e.g. by means of the method [32]. But then in contrast, we already reparameterize the resulting planar multi-patch parameterization by an AS-G^1 planar multi-patch geometry e.g. by using the technique [19]. Let $\widetilde{\mathbf{F}}$ now be the constructed AS-G^1 planar multi-patch parameterization with the single surface patch parameterizations $\widetilde{\mathbf{F}}^{(i)}$, $i \in \mathcal{I}_\Omega$, then we obtain by $\mathbf{F}^{(i)} = \mathbf{S} \circ \widetilde{\mathbf{F}}^{(i)}$, $i \in \mathcal{I}_\Omega$, an AS-G^1 multi-patch surface $\mathbf{F}$. In the following example, we demonstrate the potential of this simplified design method.

Example 2. Let $\mathbf{S}$ be the surface

$$\mathbf{S}(u_1, u_2) = \begin{bmatrix} u_1 & u_2 & 1 - u_1^2 - u_2^2 \end{bmatrix}^T \tag{16}$$

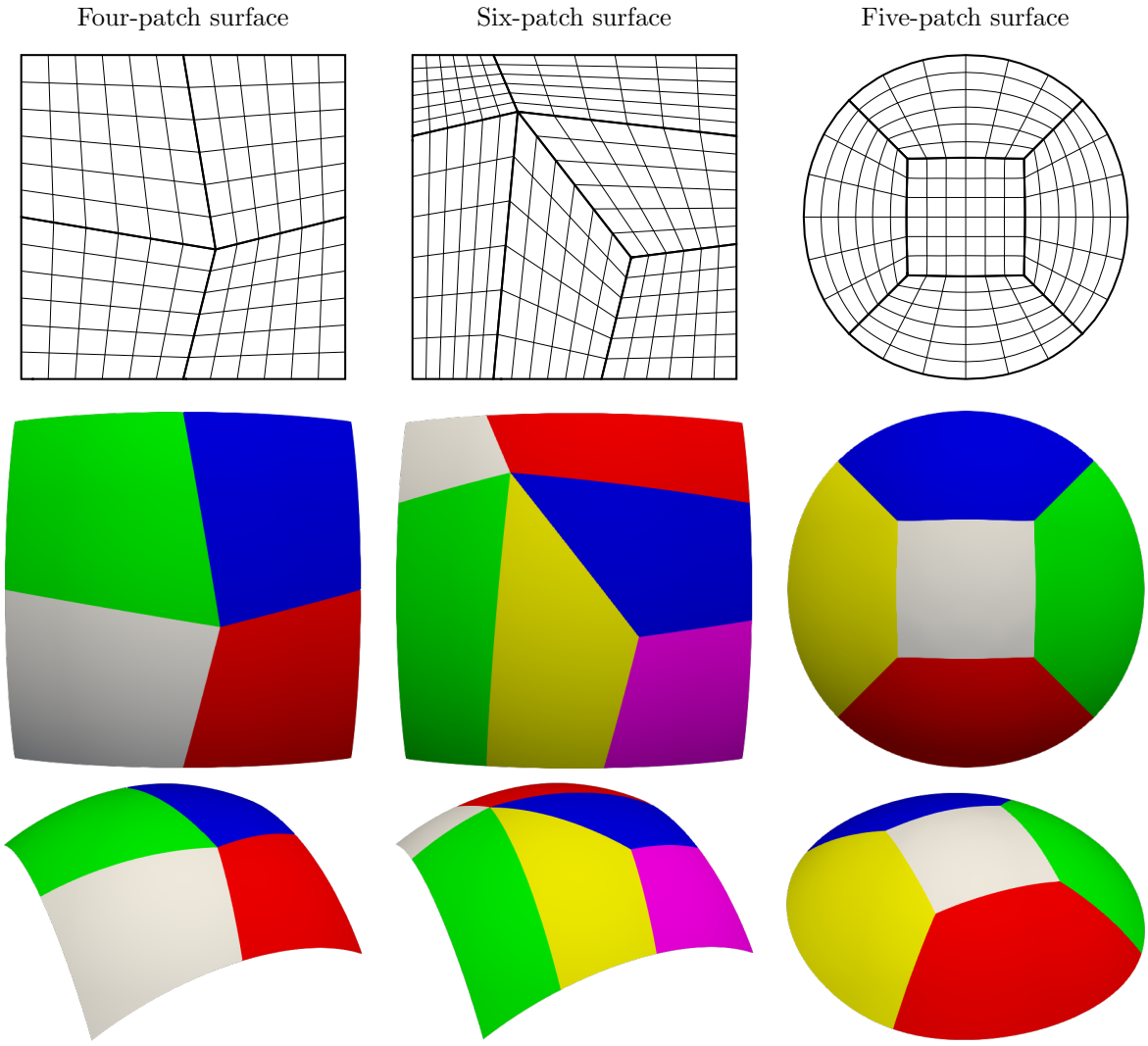

Figure 5: Example 1. Design of three different AS-G^1 multi-patch surfaces which approximate a portion of a sphere. First row: Associated planar multi-patch domains. Second and third row: Two views of the resulting AS-G^1 multi-patch surfaces.

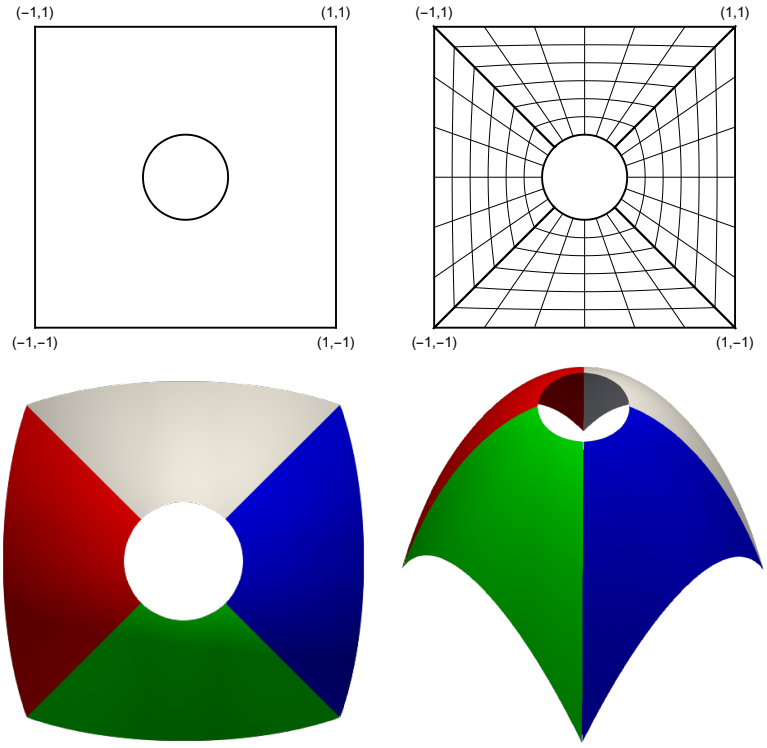

Figure 6: Example 2. Design of an AS-G^1 four-patch surface from a trimmed surface. First row: Trimmed and untrimmed parameter domain. Second row: Two views of the resulting AS-G^1 four-patch surface.

given with respect to the parameter domain $D = [-1, 1]^2$. We consider the trimmed surface $\mathbf{S}_t$, which is defined via the surface $\mathbf{S}$ and the trimmed parameter domain D_t obtained by cutting out from the parameter domain D an approximated disk whose boundary is represented by a B-spline curve of degree 2, see Figure 6 (first row, left). From the trimmed parameter domain D_t, we construct an untrimmed parameter domain described by a planar AS-G^1 four-patch parameterization $\widetilde{\mathbf{F}}$, consisting of the four-patch parameterizations $\widetilde{\mathbf{F}}^{(i)}$, $i = 1, \ldots, 4$, with $\widetilde{\mathbf{F}}^{(i)} \in (\mathcal{S}_h^{\mathbf{p},\mathbf{r}})^2$, $\mathbf{p} = (2, 2)$, $\mathbf{r} = (1, 1)$ and $h = \frac{1}{4}$, see Figure 6 (first row, right). The untrimmed parameter domain then defines an AS-G^1 four-patch parameterization $\mathbf{F}$ consisting of the single surface patch parameterizations $\mathbf{F}^{(i)} = \mathbf{S} \circ \widetilde{\mathbf{F}}^{(i)}$, $i = 1, \ldots, 4$, with $\mathbf{F}^{(i)} \in (\mathcal{S}_h^{\mathbf{p},\mathbf{r}})^3$, $\mathbf{p} = (4, 4)$, $\mathbf{r} = (1, 1)$ and $h = \frac{1}{4}$, see Figure 6 (second row). In Example 4, we will solve the biharmonic equation over the constructed AS-G^1 multi-patch surface $\mathbf{F}$.

5. Numerical experiments

We employ the C^1-smooth isogeometric functions from Section 3 to solve the biharmonic equation over different AS-G^1 multi-patch surfaces (see Examples 3–6 in Section 5.2), where we revisit the AS-G^1 multi-patch surfaces constructed in Example 1 and 2 in Section 4. In doing so, we will demonstrate on the one hand the potential of the generated C^1-smooth isogeometric functions to solve fourth order partial differential equations over multi-patch

surfaces and will numerically investigate on the other hand the approximation properties of the associated C^1-smooth space $\mathcal{A}$. For this purpose, we study before in Section 5.1 two slightly different model problems of the biharmonic equation which are adopted according to whether an open or closed multi-patch surface is used, and present for these problems an isogeometric Galerkin discretization using the constructed globally C^1-smooth functions.

5.1. Biharmonic equation & isogeometric Galerkin discretization

The proposed Galerkin discretization for solving the biharmonic equation over an open or closed multi-patch surface is based on the one in [2], but generalizes this approach in two directions: On the one hand, we have to deal with multi-patch surfaces, and on the other hand, we have to handle non-homogeneous boundary conditions for some examples. For this, we distinguish between the case of an open and closed multi-patch surface.

5.1.1. The model problem for open surfaces

In case of an open surface (Examples 3–5), we deal with the biharmonic equation possessing some specified boundary conditions. The considered problem in strong form reads as: Find $u : \Omega \to \mathbb{R}$ such that

$$\begin{cases} \Delta_\Omega^2 u(\mathbf{x}) = f(\mathbf{x}), & \mathbf{x} \in \Omega, \\ u(\mathbf{x}) = g_1(\mathbf{x}), & \mathbf{x} \in \partial\Omega, \\ \partial_{\mathbf{n}} u(\mathbf{x}) = g_2(\mathbf{x}), & \mathbf{x} \in \partial\Omega, \end{cases} \tag{17}$$

where $\partial_{\mathbf{n}} u = \nabla_\Omega u \cdot \mathbf{n}$ is the normal derivative and $\mathbf{n}$ is the outward unit normal vector on the boundary $\partial\Omega$ which is orthogonal both to the normal vector of the surface and to the tangent vector of the boundary curve $\partial\Omega$, f is the force function in Ω and g_1 and g_2 are two functions given on the boundary $\partial\Omega$ describing the boundary conditions for u and $\partial_{\mathbf{n}} u$, respectively. The weak formulation of the problem (17) is to find $u \in H_g^2(\Omega)$ such that

$$a(u, v_0) = F(v_0), \quad \text{for all } v_0 \in H_0^2(\Omega), \tag{18}$$

where a is a bilinear form and F is a linear functional, of the form

$$a \,:\, H_g^0(\Omega) \times H_0^2 \to \mathbb{R}, \quad a(u, v_0) = \int_\Omega \Delta_\Omega u(\mathbf{x}) \Delta_\Omega v_0(\mathbf{x})\, d\Omega,$$

and

$$F \,:\, H_0^2(\Omega) \to \mathbb{R}, \quad F(v_0) = \int_\Omega f(\mathbf{x}) v_0(\mathbf{x})\, d\Omega,$$

respectively, and where the spaces $H_g^2(\Omega)$ and $H_0^2(\Omega)$ are given as

$$H_g^2(\Omega) = \left\{ v \in H^2(\Omega) \mid v(\mathbf{x}) = g_1(\mathbf{x}) \text{ and } \partial_{\mathbf{n}} v(\mathbf{x}) = g_2(\mathbf{x}) \text{ for } \mathbf{x} \in \partial\Omega \right\}$$

and

$$H_0^2(\Omega) = \left\{ v \in H^2(\Omega) \mid v(\mathbf{x}) = 0 \text{ and } \partial_{\mathbf{n}} v(\mathbf{x}) = 0 \text{ for } \mathbf{x} \in \partial\Omega \right\},$$

respectively. Problem (18) is equivalent to compute $u = u_g + u_0$, with $u_g \in H^2_g(\Omega)$ arbitrary but fixed and $u_0 \in H^2_0(\Omega)$ to be determined, such that

$$a(u_0, v_0) = F(v_0) - a(u_g, v_0), \quad \text{for all } v_0 \in H^2_0(\Omega). \tag{19}$$

We now apply Galerkin projection to the problem (19) by using the C^1-smooth space $\mathcal{A}$, and denote below this C^1-smooth space by $\mathcal{A}_h$ to specify the selected mesh size h. For this purpose, we first decompose the space $\mathcal{A}_h$ into the direct sum

$$\mathcal{A}_h = \mathcal{A}_{h,g} \oplus \mathcal{A}_{h,0}$$

with

$$\mathcal{A}_{h,0} = \{v_h \in \mathcal{A}_h \mid v_h = 0 \text{ and } \partial_{\mathbf{n}} v_h = 0 \text{ on } \partial\Omega\}.$$

Then, the problem is to find $u_h = u_{h,g} + u_{h,0}$ with $u_{h,g} \in \mathcal{A}_{h,g}$ and $u_{h,0} \in \mathcal{A}_{h,0}$ by computing first $u_{h,g} \in \mathcal{A}_{h,g}$ via the quadratic minimization problem

$$\int_{\partial\Omega} (u_{h,g}(\mathbf{x}) - g_1(\mathbf{x}))^2 \, d\partial\Omega + \omega \int_{\partial\Omega} (\partial_{\mathbf{n}} u_{h,g}(\mathbf{x}) - g_2(\mathbf{x}))^2 \, d\partial\Omega \to \min_{u_{h,g} \in \mathcal{A}_{h,g}},$$

with a suitable non-negative weight ω, and determining afterwards $u_{h,0} \in \mathcal{A}_{h,0}$ via the variational problem

$$a(u_{h,0}, v_{h,0}) = F(v_{h,0}) - a(u_{h,g}, v_{h,0}), \quad \text{for all } v_{h,0} \in \mathcal{A}_{h,0}. \tag{20}$$

Let us study the variational problem (20) in more detail. Assuming that $\{\phi_{h,j}\}_{j \in \mathcal{J}}$ with $\mathcal{J} = \{1, \ldots, \dim \mathcal{A}_{h,0}\}$ is a basis of the C^1-smooth space $\mathcal{A}_{h,0}$, the variational problem (20) is equal to solve the linear system $K\mathbf{c} = \mathbf{f}$ for the coefficients $\mathbf{c} = (c_j)_{j \in \mathcal{J}}$ of

$$u_{h,0}(\mathbf{x}) = \sum_{j \in \mathcal{J}} c_j \phi_{h,j}(\mathbf{x}), \quad \mathbf{x} \in \Omega,$$

where the elements of the stiffness matrix $K = (k_{j_1,j_2})_{j_1,j_2 \in \mathcal{J}}$ and of the load vector $\mathbf{f} = (f_j)_{j \in \mathcal{J}}$ are given by

$$k_{j_1,j_2} = \int_\Omega \Delta_\Omega \phi_{h,j_1}(\mathbf{x}) \Delta_\Omega \phi_{h,j_2}(\mathbf{x}) d\Omega,$$

and

$$f_j = \int_\Omega f(\mathbf{x}) \phi_{j,h}(\mathbf{x}) \, d\Omega,$$

respectively. Since Ω is a multi-patch surface domain given by $\Omega = \cup_{i \in \mathcal{I}_\Omega} \overline{\Omega^{(i)}}$, the elements k_{j_1,j_2} and f_j can be also computed via

$$k_{j_1,j_2} = \sum_{i \in \mathcal{I}_\Omega} \int_{\Omega^{(i)}} \Delta_\Omega \phi_{h,j_1}(\mathbf{x}) \Delta_\Omega \phi_{h,j_2}(\mathbf{x}) d\Omega^{(i)},$$

and

$$f_j = \sum_{i \in \mathcal{I}_\Omega} \int_{\Omega^{(i)}} f(\mathbf{x}) \phi_{j,h}(\mathbf{x}) \, d\Omega^{(i)},$$

respectively. By using the relations $\psi_{h,j}^{(i)}(\boldsymbol{\xi}) = \left(\phi_{h,j} \circ \mathbf{F}^{(i)}\right)(\boldsymbol{\xi})$, $i \in \mathcal{I}_\Omega$, $j \in \mathcal{J}$ and $\widetilde{f}^{(i)}(\boldsymbol{\xi}) = \left(f \circ \mathbf{F}^{(i)}\right)(\boldsymbol{\xi})$, $i \in \mathcal{I}_\Omega$, and the tools discussed in Section 2.3, the isogeometric formulation of the entries k_{j_1,j_2}, $j_1, j_2 \in \mathcal{J}$, and f_j, $j \in \mathcal{J}$, are given by

$$k_{j_1,j_2} = \sum_{i \in \mathcal{I}_\Omega} \int_{[0,1]^2} \frac{1}{g^{(i)}(\boldsymbol{\xi})} \nabla_{\boldsymbol{\xi}} \cdot \left((G_0^{(i)})^{-1}(\boldsymbol{\xi}) \nabla_{\boldsymbol{\xi}} \psi_{h,j_1}^{(i)}(\boldsymbol{\xi}) \right) \nabla_{\boldsymbol{\xi}} \cdot \left((G_0^{(i)})^{-1}(\boldsymbol{\xi}) \nabla_{\boldsymbol{\xi}} \psi_{h,j_2}^{(i)}(\boldsymbol{\xi}) \right) d\boldsymbol{\xi},$$

and

$$f_j = \sum_{i \in \mathcal{I}_\Omega} \int_{[0,1]^2} \widetilde{f}^{(i)}(\boldsymbol{\xi}) \psi_{h,j}^{(i)}(\boldsymbol{\xi}) g^{(i)}(\boldsymbol{\xi}) \, d\boldsymbol{\xi},$$

respectively.

5.1.2. The model problem for closed surfaces

In case of closed surfaces (Example 6), we consider instead of problem (17) the following biharmonic equation in strong form: Find $u : \Omega \to \mathbb{R}$ such that

$$\Delta_\Omega^2 \, u(\mathbf{x}) + \lambda u(\mathbf{x}) = f(\mathbf{x}), \quad \mathbf{x} \in \Omega. \tag{21}$$

The reason for this is that in case of closed surfaces boundary conditions cannot be imposed because there is no boundary. Note that adding the extra term λu, with $\lambda > 0$, is necessary to guarantee the well-posedness of the problem (21), cf. [2]. Let us study now the derivation of the isogeometric Galerkin discretization of the problem (21), which proceeds slightly different to the problem (17) for the case of open surfaces. We start with the weak formulation of the problem (21), which is to find $u \in H^2(\Omega)$ such that

$$a(u, v) = F(v), \quad \forall v \in H^2(\Omega), \tag{22}$$

where again a is a bilinear form and F is a linear functional, but now of the form

$$a \, : \, H^2(\Omega) \times H^2(\Omega) \to \mathbb{R}, \quad a(u, v) = \int_\Omega \Delta_\Omega u(\mathbf{x}) \Delta_\Omega v(\mathbf{x}) \, d\Omega + \int_\Omega \lambda u(\mathbf{x}) v(\mathbf{x}) \, d\Omega,$$

and

$$F \, : \, H^2(\Omega) \to \mathbb{R}, \quad F(v) = \int_\Omega f(\mathbf{x}) v(\mathbf{x}) \, d\Omega,$$

respectively. We then also apply Galerkin projection to the problem (22) by using the C^1-smooth space $\mathcal{A}$, again denoted by $\mathcal{A}_h$, which leads to: Find $u_h \in \mathcal{A}_h$ such that

$$a(u_h, v_h) = F(v_h), \quad \text{for all } v_h \in \mathcal{A}_h. \tag{23}$$

Assuming that $\{\phi_{h,j}\}_{j \in \mathcal{J}}$ with $\mathcal{J} = \{1, \ldots, \dim \mathcal{A}_h\}$ is a basis of the C^1-smooth space $\mathcal{A}_h$, problem (23) is again equivalent to a linear system $K\mathbf{c} = \mathbf{f}$, now for coefficients $\mathbf{c} = (c_j)_{j \in \mathcal{J}}$ of

$$u_h(\mathbf{x}) = \sum_{j \in \mathcal{J}} c_j \phi_{h,j}(\mathbf{x}), \quad \mathbf{x} \in \Omega,$$

for a stiffness matrix $K = (k_{j_1,j_2})_{j_1,j_2 \in \mathcal{J}}$ with the elements

$$k_{j_1,j_2} = \int_\Omega \Delta_\Omega \phi_{h,j_1}(\mathbf{x}) \Delta_\Omega \phi_{h,j_2}(\mathbf{x}) d\Omega + \int_\Omega \lambda \phi_{h,j_1}(\mathbf{x}) \phi_{h,j_2}(\mathbf{x}) d\Omega,$$

and for a load vector $\mathbf{f} = (f_j)_{j \in \mathcal{J}}$ with the elements

$$f_j = \int_\Omega f(\mathbf{x}) \phi_{j,h}(\mathbf{x})\, d\Omega.$$

Again, due to the fact that Ω is a multi-patch surface domain given by $\Omega = \cup_{i \in \mathcal{I}_\Omega} \overline{\Omega^{(i)}}$, and using the relations $\psi_{h,j}^{(i)}(\boldsymbol{\xi}) = \left(\phi_{h,j} \circ \mathbf{F}^{(i)}\right)(\boldsymbol{\xi})$, $i \in \mathcal{I}_\Omega$, $j \in \mathcal{J}$ and $\widetilde{f}^{(i)}(\boldsymbol{\xi}) = \left(f \circ \mathbf{F}^{(i)}\right)(\boldsymbol{\xi})$, $i \in \mathcal{I}_\Omega$, and the tools discussed in Section 2.3, we can express the isogeometric formulation of the elements k_{j_1,j_2}, $j_1, j_2 \in \mathcal{J}$, and f_j, $j \in \mathcal{J}$, which possess now the form

$$\begin{aligned} k_{j_1,j_2} &= \sum_{i \in \mathcal{I}_\Omega} \int_{[0,1]^2} \frac{1}{g^{(i)}(\boldsymbol{\xi})} \nabla_{\boldsymbol{\xi}} \cdot \left((G_0^{(i)})^{-1}(\boldsymbol{\xi}) \nabla_{\boldsymbol{\xi}} \psi_{h,j_1}^{(i)}(\boldsymbol{\xi}) \right) \nabla_{\boldsymbol{\xi}} \cdot \left((G_0^{(i)})^{-1}(\boldsymbol{\xi}) \nabla_{\boldsymbol{\xi}} \psi_{h,j_2}^{(i)}(\boldsymbol{\xi}) \right) d\boldsymbol{\xi} \\ &+ \sum_{i \in \mathcal{I}_\Omega} \int_{[0,1]^2} \lambda \psi_{h,j_1}^{(i)}(\boldsymbol{\xi}) \psi_{h,j_2}^{(i)}(\boldsymbol{\xi}) g^{(i)}(\boldsymbol{\xi})\, d\boldsymbol{\xi}, \end{aligned}$$

and

$$f_j = \sum_{i \in \mathcal{I}_\Omega} \int_{[0,1]^2} \widetilde{f}^{(i)}(\boldsymbol{\xi}) \psi_{h,j}^{(i)}(\boldsymbol{\xi}) g^{(i)}(\boldsymbol{\xi})\, d\boldsymbol{\xi},$$

respectively.

5.2. Numerical examples

We demonstrate the potential of the C^1-smooth isogeometric functions, constructed in Section 3, to solve a fourth order partial differential equation, namely the biharmonic equation, over different AS-G^1 multi-patch surfaces by means of isogeometric analysis. For this purpose, we use the isogeometric Galerkin discretization of the biharmonic equation from Section 5.1.1 or 5.1.2 depending on considering an open or closed multi-patch surface, respectively, and perform several experiments to numerically investigate the approximation properties of the C^1 isogeometric spline spaces, see Examples 3–6, below. The construction of the employed AS-G^1 multi-patch surfaces is based on different design methods, namely on the techniques developed in Section 4 (Example 4 and 5), on the method [19] (Example 6) or on a simple design approach directly introduced in the corresponding example (Example 3). For the numerical study of the approximation properties of the C^1 isogeometric spline spaces $\mathcal{A}$ over the different AS-G^1 multi-patch surfaces, we perform for all examples h-refinement to generate a sequence of C^1 isogeometric spline spaces $\mathcal{A}$ with mesh sizes $h = 2^{-L} h_0$, denoted as in Section 5.1 by $\mathcal{A}_h$, where h_0 is the initial mesh size and $L = 0, 1, 2, \ldots$ is the level of refinement.

The resulting errors for solving the biharmonic equation are computed in two different ways depending on whether or not the exact solution of the considered problem is available.

In case one global parameterization of the considered AS-G^1 multi-patch surface exists, as in Example 3 and 4, we use an exact solution u_{ex}, in our instances the analytic function

$$u_{ex}(x_1, x_2, x_3) = 2\cos(8x_1)\cos(1 - 6x_2), \tag{24}$$

to determine the functions f, g_1 and g_2 of the problem (17). Then, we compute for each mesh size h just relative errors, namely in our case the L^2-norm

$$\frac{\|u_h - u_{ex}\|_{L^2}}{\|u_{ex}\|_{L^2}}, \tag{25}$$

the H^1-seminorm

$$\frac{|u_h - u_{ex}|_{H^1}}{|u_{ex}|_{H^1}} \tag{26}$$

and the L^2-norm of the difference of the Laplacian

$$\frac{\|\Delta u_h - \Delta u_{ex}\|_{L^2}}{\|\Delta u_{ex}\|_{L^2}}, \tag{27}$$

which is equivalent to the H^2-seminorm [2]. Below, we will refer for the sake of brevity to the equivalent norm (27) just as H^2-seminorm.

In case one global parameterization of the considered AS-G^1 multi-patch surface does not exist as in Example 5 and 6, and additionally in Example 4 for comparison, we perform $h - h/2$ type error estimation (see e.g. [8, 10]), performing the difference between two subsequent computed solutions at the mesh size h and $h/2$. In particular, the estimators have the form

$$\|u_h - u_{h/2}\|_{L^2}, \quad |u_h - u_{h/2}|_{H^1} \quad \text{and} \quad \|\Delta u_h - \Delta u_{h/2}\|_{L^2}. \tag{28}$$

These error estimators can be seen as the analogues of the relative errors defined in (25), (26) and (27), respectively. Note that the last estimator in (28) is again equivalent to the estimator $|u_h - u_{h/2}|_{H^2}$. For the sake of brevity, we refer to the error estimators (28) in the figures of the concrete examples below just by L^2, H^1 and H^2.

While in Example 4 and Example 5 for open surfaces, we solve the problem (17) by choosing the values of the right hand side f and of the two boundary value functions g_1 and g_2 as

$$f = 5, \quad g_1 = 0 \quad \text{and} \quad g_2 = 0, \tag{29}$$

respectively, we solve in Example 6 for the considered closed surface the model problem described in (21) for the function

$$f(x_1, x_2, x_3) = \cos\left(\frac{\pi}{2}x_1\right)\cos\left(\frac{\pi}{2}x_2\right)\cos\left(\frac{\pi}{2}x_3\right). \tag{30}$$

Let us study now in detail the Examples 3–6, where the numerical results will indicate in all four cases optimal approximation properties of the corresponding C^1-smooth isogeometric spline spaces $\mathcal{A}_h$. In the first three examples, we deal with the case open AS-G^1 multi-patch surfaces and solve the biharmonic equation over these surfaces.

Example 3. We consider from Example 2 the surface $\mathbf{S}$ given by (16), but now with respect to three different parameter domains represented by planar bilinear multi-patch parameterizations $\widetilde{\mathbf{F}}_\ell$, $\ell = 1, 2, 3$, where $\widetilde{\mathbf{F}}_1$, $\widetilde{\mathbf{F}}_2$ and $\widetilde{\mathbf{F}}_3$ is the three-, four- and five-patch domain, respectively, given in Figure 7 (first row). More precisely, we generate the three multi-patch surfaces $\mathbf{F}_\ell$, $\ell = 1, 2, 3$, where $\mathbf{F}_1$, $\mathbf{F}_2$ and $\mathbf{F}_3$ is the three-, four- and five-patch surface, respectively, consisting of the single surface patch parameterizations $\mathbf{F}_\ell^{(i)} = \mathbf{S} \circ \widetilde{\mathbf{F}}_\ell^{(i)}$, $i = 1, \dots, 2 + \ell$, see Figure 7 (second row). The resulting multi-patch surfaces $\mathbf{F}_\ell$, $\ell = 1, 2, 3$, are trivially AS-G^1 by construction, and possess surface patch parameterizations $\mathbf{F}_\ell^{(i)} \in (\mathcal{P}_2^{\mathbf{q}})^3$, $i = 1, \dots, 2 + \ell$, with $\mathbf{q} = (2, 2)$. We solve the biharmonic equation (17) for the functions f, g_1 and g_2 obtained by the exact solution (24), see Figure 7 (third row), over the three multi-patch surfaces $\mathbf{F}_\ell$, $\ell = 1, 2, 3$, by using the C^1-smooth spaces $\mathcal{A}_h$ for $p = 3, 4$ and $r = 1$. The numerical results u_h indicate optimal rates of convergence in the L^2 norm and in the H^1 and H^2 seminorms as shown in Figure 7 (fourth row) for degree $p = 3$ and in Figure 7 (fifth row) for degree $p = 4$.

Example 4. Let $\mathbf{F}$ be the AS-G^1 four-patch surface from Example 2 visualized in Figure 6 (second row), which has been constructed from a trimmed surface and which consists of surface patch parameterizations $\mathbf{F}^{(i)} \in (\mathcal{S}_h^{\mathbf{p},\mathbf{r}})^3$, $i = 1, \dots, 4$, $\mathbf{p} = (4, 4)$, $\mathbf{r} = (1, 1)$ and $h = \frac{1}{4}$. We solve now the biharmonic equation (17) over the AS-G^1 four-patch surface $\mathbf{F}$ for two different settings by using the C^1-smooth space $\mathcal{A}_h$ for $p = 4$ and $r = 1$. While the functions f, g_1 and g_2 are derived in the first case from the exact solution (24), they are given in the second case as in (29). In Figure 8 (first row), the numerical results u_h are visualized at the finest selected mesh size of $\mathcal{A}_h$ for the first case on the left side and for the second case on the right side. In both cases, the obtained convergence results indicate optimal rates in the L^2 norm and in the H^1 and H^2 seminorms as shown in Figure 8 (second row) with the first case on the left side and with the second case on the right side.

Example 5. We consider the three AS-G^1 multi-patch surfaces $\mathbf{F}_\ell$, $\ell = 1, 2, 3$, constructed in Example 1 and shown in Figure 5 (second row, from left to right), which approximate in each case a portion of a sphere and consist of four, six and five surface patch parameterizations $\mathbf{F}_\ell^{(i)} \in (\mathcal{S}_h^{\mathbf{p},\mathbf{r}})^3$, $\mathbf{p} = (3, 3)$, $\mathbf{r} = (1, 1)$ and $h = \frac{1}{3}$, respectively. We solve over these AS-G^1 multi-patch surfaces the biharmonic problem (17) with the right hand side and boundary conditions (29) by using C^1-smooth isogeometric spline spaces $\mathcal{A}_h$ for degree $p = 3$ and $r = 1$. In all three instances, the numerical results u_h, which are are visualized at the finest selected mesh size of $\mathcal{A}_h$ in Figure 9 (first row), indicate optimal convergence rates in the L^2 norm and in the H^1 and H^2 seminorms as shown in Figure 9 (second row).

In the last example, we deal with the case of a closed AS-G^1 multi-patch surface and solve the biharmonic equation over this surface.

Example 6. We consider the closed AS-G^1 six-patch surface $\mathbf{F}$ from [19, Example 5], which is a multi-patch spline approximation of a sphere, where the single patch parameterizations $\mathbf{F}^{(i)}$, $i = 1, \dots, 6$, belong to the space $(\mathcal{S}_h^{\mathbf{p},\mathbf{r}})^3$ with $\mathbf{p} = (3, 3)$, $\mathbf{r} = (1, 1)$ and $h = \frac{1}{2}$, see Figure 10 (first row). We solve the biharmonic equation (21) for the parameter $\lambda = 1$

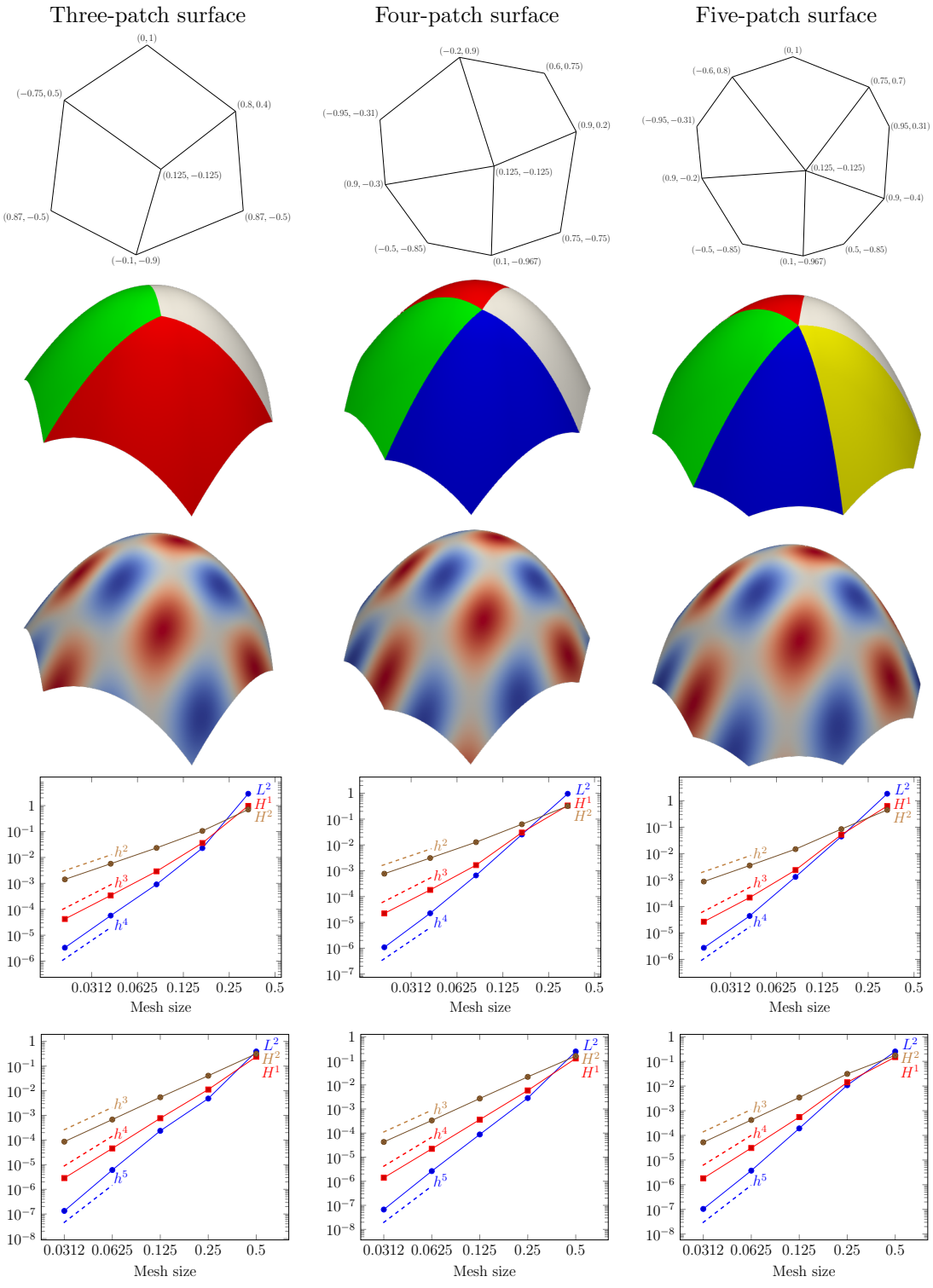

Figure 7: Example 3. Solving the biharmonic equation (17) over three different AS-G^1 multi-patch surfaces. First row: Parameter domains. Second row: AS-G^1 multi-patch surfaces. Third row: Exact solutions (24). Fourth and fifth row: Convergence plots by using the C^1-smooth space $\mathcal{A}_h$ for degree $p = 3$ (fourth row) and $p = 4$ (fifth row) and regularity $r = 1$ in both cases.

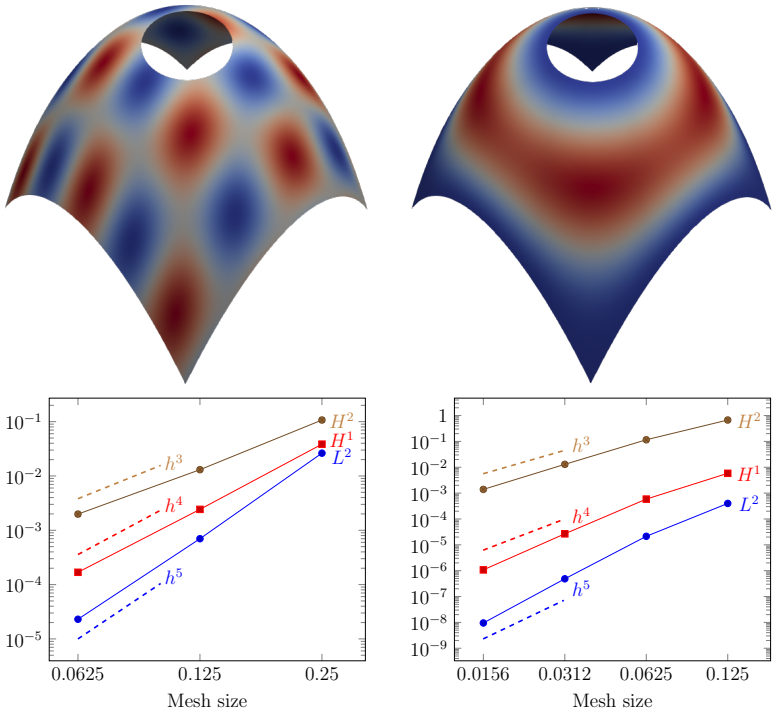

Figure 8: Example 4. Solving the biharmonic equation (17) over the AS-G^1 four-patch surface from Example 2 shown in Figure 6 (second row). First and second row: The numerical results u_h at the finest selected mesh size h and the resulting convergence plots for solving the biharmonic equation (17) for the functions f, g_1 and g_2 derived from the exact solution (24) (left) and given as in (29) (right) using the C^1-smooth space $\mathcal{A}_h$ for degree $p = 4$ and regularity $r = 1$.

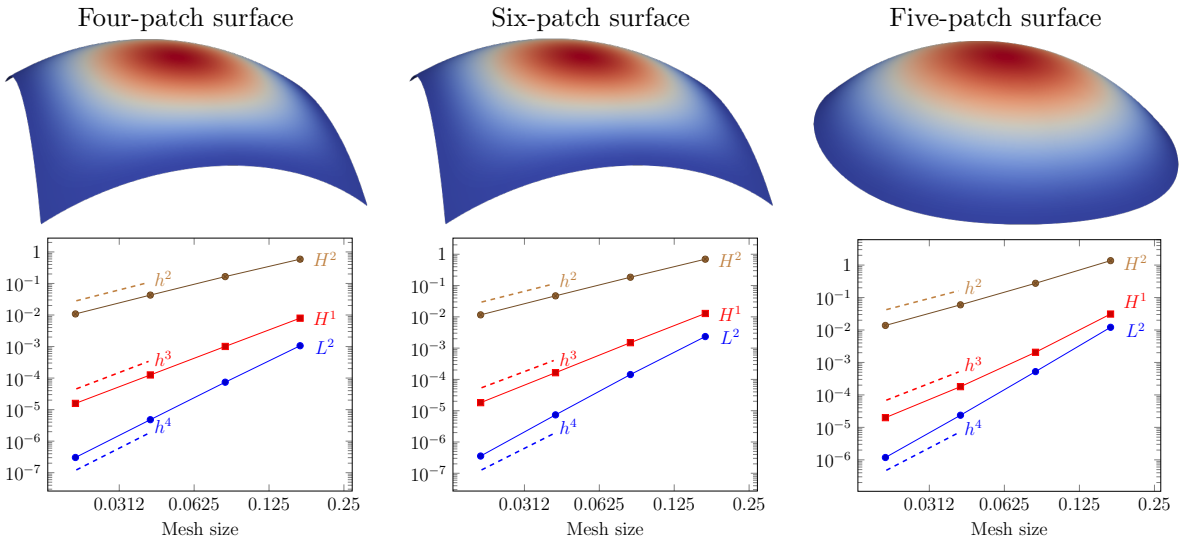

Figure 9: Example 5. Solving the biharmonic equation (17) over the three different AS-G^1 multi-patch surfaces constructed in Example 1 and visualized in Figure 5 (second row), which approximate in each case a portion of a sphere. First and second row: The numerical results u_h at the finest selected mesh size h and the resulting convergence plots for solving the biharmonic equation (17) using the C^1-smooth space $\mathcal{A}_h$ for degree $p = 3$ and regularity $r = 1$.

and the function f as given in (30) over the closed AS-G^1 six-patch surface $\mathbf{F}$ by using the C^1-smooth space $\mathcal{A}_h$ for $p = 3$ and $r = 1$. Also in this case of a closed AS-G^1 multi-patch surface, the numerical results u_h, see Figure 10 (second row, left) for the finest selected mesh size h, indicate optimal rates of convergence in the L^2 norm and in the H^1 and H^2 seminorms, see Figure 10 (second row, right).

6. Conclusion

We presented the construction of a particular C^1-smooth isogeometric spline space $\mathcal{A}$ defined over an AS-G^1 multi-patch surface or equivalently over its AS-G^1 skeleton. Our method extends the construction [20, 21], which is limited to the case of AS-G^1 planar multi-patch geometries, to the case of AS-G^1 multi-patch surfaces. The constructed C^1-smooth isogeometric spline space $\mathcal{A}$ is a subspace of the full C^1-smooth space $\mathcal{V}^1$, which is simple to generate, possesses an explicitly given, locally supported basis and whose dimension is independent of the underlying AS-G^1 parameterization of the multi-patch surface.

The presented numerical examples of solving the biharmonic equation over different AS-G^1 multi-patch surfaces with the resulting optimal convergence rates in the L^2 norm and in the H^1 and H^2 seminorms indicate that the constructed C^1-smooth space $\mathcal{A}$ possesses optimal approximation properties. We further developed simple and practical methods for the design of AS-G^1 multi-patch surfaces, which allow the approximation of (approximately) smooth surfaces by AS-G^1 multi-patch surfaces, and introduced an isogeometric

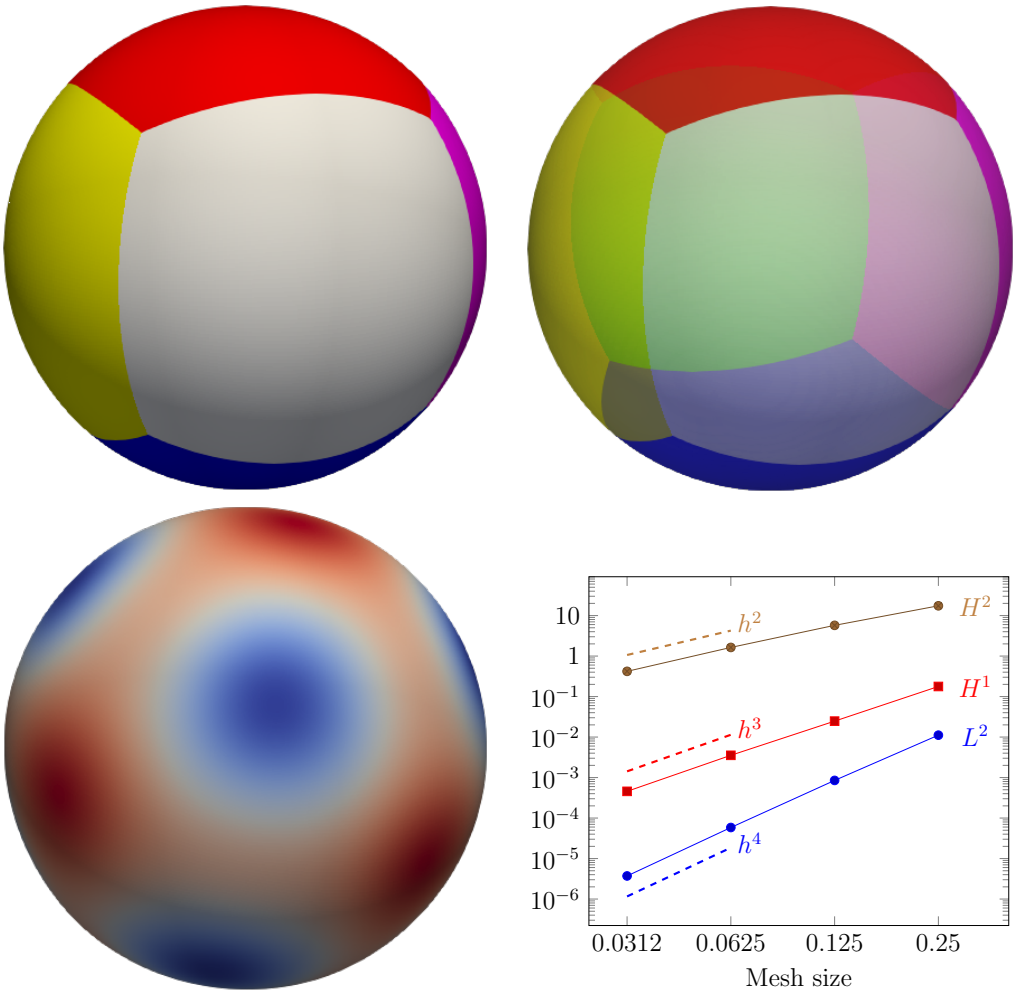

Figure 10: Example 6. Solving the biharmonic equation (21) over an AS-G^1 six-patch surface approximating a sphere (first row) with the numerical result u_h at the finest selected mesh size h (second row, left) and the resulting convergence plot (second row, right) using the C^1-smooth space $\mathcal{A}_h$ for degree $p = 3$ and regularity $r = 1$.

multi-patch Galerkin discretization of the considered biharmonic problem.

A first interesting topic for possible future research is the use of the constructed C^1-smooth isogeometric spline space $\mathcal{A}$ to solve further fourth order problems such as the Kirchhoff-Love shell problem, the Cahn-Hilliard equation or problems of strain gradient elasticity. Another possible topic is the detailed study and construction of AS-G^1 template multi-patch parameterizations as well as of their AS-G^1 skeletons in the presented general framework for the design of AS-G^1 multi-patch surfaces to provide the framework for a large class of initial surfaces.

Acknowledgments. This research has been supported by the Austrian Science Fund (FWF) through the project P 33023.

References

[1] F. Auricchio, L. Beirão da Veiga, A. Buffa, C. Lovadina, A. Reali, and G. Sangalli. A fully "locking-free" isogeometric approach for plane linear elasticity problems: a stream function formulation. *Comput. Methods Appl. Mech. Engrg.*, 197(1):160–172, 2007.

[2] A. Bartezzaghi, L. Dedè, and A. Quarteroni. Isogeometric analysis of high order partial differential equations on surfaces. *Computer Methods in Applied Mechanics and Engineering*, 295:446–469, 2015.

[3] L. Beirão da Veiga, A. Buffa, G. Sangalli, and R. Vázquez. Mathematical analysis of variational isogeometric methods. *Acta Numerica*, 23:157–287, 5 2014.

[4] D. J. Benson, Y. Bazilevs, M.-C. Hsu, and T. J.R. Hughes. A large deformation, rotation-free, isogeometric shell. *Comput. Methods Appl. Mech. Engrg.*, 200(13):1367–1378, 2011.

[5] C.L. Chan, C. Anitescu, and T. Rabczuk. Isogeometric analysis with strong multipatch C^1-coupling. *Comput. Aided Geom. Design*, 62:294–310, 2018.

[6] A. Collin, G. Sangalli, and T. Takacs. Analysis-suitable G^1 multi-patch parametrizations for C^1 isogeometric spaces. *Comput. Aided Geom. Des.*, 47:93 – 113, 2016.

[7] J. A. Cottrell, T. J. R. Hughes, and Y. Bazilevs. *Isogeometric Analysis: Toward Integration of CAD and FEA*. John Wiley & Sons, Chichester, England, 2009.

[8] C. Erath, G. Gantner, and D. Praetorius. Optimal convergence behavior of adaptive FEM driven by simple $(h - h/2)$-type error estimators. *Comput. Math. Appl.*, 79(3):623–642, 2020.

[9] G. Farin. *Curves and Surfaces for Computer-Aided Geometric Design*. Academic Press, 1997.

[10] S. Ferraz-Leite, C. Ortner, and D. Praetorius. Convergence of simple adaptive Galerkin schemes based on $(h - h/2)$ error estimators. *Numer. Math.*, 116(2):291–316, 2010.

[11] P. Fischer, M. Klassen, J. Mergheim, P. Steinmann, and R. Müller. Isogeometric analysis of 2D gradient elasticity. *Comput. Mech.*, 47(3):325–334, 2011.

[12] H. Gómez, V. M Calo, Y. Bazilevs, and T. J.R. Hughes. Isogeometric analysis of the Cahn–Hilliard phase-field model. *Comput. Methods Appl. Mech. Engrg.*, 197(49):4333–4352, 2008.

[13] H. Gomez, V. M. Calo, and T. J. R. Hughes. Isogeometric analysis of Phase–Field models: Application to the Cahn–Hilliard equation. In *ECCOMAS Multidisciplinary Jubilee Symposium: New Computational Challenges in Materials, Structures, and Fluids*, pages 1–16. Springer Netherlands, 2009.

[14] D. Groisser and J. Peters. Matched G^k-constructions always yield C^k-continuous isogeometric elements. *Comput. Aided Geom. Des.*, 34:67 – 72, 2015.

[15] J. Hoschek and D. Lasser. *Fundamentals of computer aided geometric design*. A K Peters Ltd., Wellesley, MA, 1993.

[16] T. J. R. Hughes, J. A. Cottrell, and Y. Bazilevs. Isogeometric analysis: CAD, finite elements, NURBS, exact geometry and mesh refinement. *Comput. Methods Appl. Mech. Engrg.*, 194(39-41):4135–4195, 2005.

[17] T. J. R. Hughes, G. Sangalli, T. Takacs, and D. Toshniwal. Chapter 8 - Smooth multi-patch discretizations in Isogeometric Analysis. In *Geometric Partial Differential Equations - Part II*, volume 22 of *Handbook of Numerical Analysis*, pages 467–543. Elsevier, 2021.

[18] M. Kapl, F. Buchegger, M. Bercovier, and B. Jüttler. Isogeometric analysis with geometrically continuous functions on planar multi-patch geometries. *Comput. Methods Appl. Mech. Engrg.*, 316:209 – 234, 2017.

[19] M. Kapl, G. Sangalli, and T. Takacs. Construction of analysis-suitable G^1 planar multi-patch parameterizations. *Computer-Aided Design*, 97:41 – 55, 2018.

[20] M. Kapl, G. Sangalli, and T. Takacs. Isogeometric analysis with C^1 functions on planar, unstructured quadrilateral meshes. *The SMAI journal of computational mathematics*, 5:67–86, 2019.

[21] M. Kapl, G. Sangalli, and T. Takacs. An isogeometric C^1 subspace on unstructured multi-patch planar domains. *Comput. Aided Geom. Des.*, 69:55–75, 2019.

[22] M. Kapl, V. Vitrih, B. Jüttler, and K. Birner. Isogeometric analysis with geometrically continuous functions on two-patch geometries. *Comput. Math. Appl.*, 70(7):1518 – 1538, 2015.

[23] K. Karčiauskas, T. Nguyen, and J. Peters. Generalizing bicubic splines for modeling and IGA with irregular layout. *Comput.-Aided Des.*, 70:23 – 35, 2016.

[24] K. Karčiauskas and J. Peters. Refinable G^1 functions on G^1 free-form surfaces. *Comput. Aided Geom. Des.*, 54:61–73, 2017.

[25] K. Karčiauskas and J. Peters. Refinable bi-quartics for design and analysis. *Comput.-Aided Des.*, pages 204–214, 2018.

[26] J. Kiendl, Y. Bazilevs, M.-C. Hsu, R. Wüchner, and K.-U. Bletzinger. The bending strip method for isogeometric analysis of Kirchhoff-Love shell structures comprised of multiple patches. *Comput. Methods Appl. Mech. Engrg.*, 199(35):2403–2416, 2010.

[27] J. Kiendl, K.-U. Bletzinger, J. Linhard, and R. Wüchner. Isogeometric shell analysis with Kirchhoff-Love elements. *Comput. Methods Appl. Mech. Engrg.*, 198(49):3902–3914, 2009.

[28] J. Kiendl, M.-Ch. Hsu, M. C. H. Wu, and A. Reali. Isogeometric Kirchhoff-Love shell formulations for general hyperelastic materials. *Comput. Methods Appl. Mech. Engrg.*, 291:280 – 303, 2015.

[29] J. Liu, L. Dedè, J. A. Evans, M. J. Borden, and T. J. R. Hughes. Isogeometric analysis of the advective Cahn–Hilliard equation: Spinodal decomposition under shear flow. *Journal of Computational Physics*, 242:321 – 350, 2013.

[30] C. Loop and S. Schaefer. Approximating Catmull-Clark subdivision surfaces with bicubic patches. *ACM Trans. Graph.*, 27(1):1–11, 2008.

[31] R. Makvandi, J. Ch. Reiher, A. Bertram, and D. Juhre. Isogeometric analysis of first and second strain gradient elasticity. *Comput. Mech.*, 61(3):351–363, 2018.

[32] F. Massarwi, B. van Sosin, and G. Elber. Untrimming: Precise conversion of trimmed surfaces to tensor-product surfaces. *Computers & Graphics*, 70:80–91, 2018.

[33] T. Nguyen, K. Karčiauskas, and J. Peters. C^1 finite elements on non-tensor-product 2d and 3d manifolds. *Applied Mathematics and Computation*, 272:148 – 158, 2016.

[34] T. Nguyen and J. Peters. Refinable C^1 spline elements for irregular quad layout. *Comput. Aided Geom. Des.*, 43:123 – 130, 2016.

[35] J. Niiranen, S. Khakalo, V. Balobanov, and A. H. Niemi. Variational formulation and isogeometric analysis for fourth-order boundary value problems of gradient-elastic bar and plane strain/stress problems. *Comput. Methods Appl. Mech. Engrg.*, 308:182–211, 2016.

[36] J. Peters. Geometric continuity. In *Handbook of computer aided geometric design*, pages 193–227. North-Holland, Amsterdam, 2002.

[37] G. Sangalli, T. Takacs, and R. Vázquez. Unstructured spline spaces for isogeometric analysis based on spline manifolds. *Computer Aided Geometric Design*, 47:61–82, 2016.